*Biochem. J.* (1976) **154**, 449–469
*Printed in Great Britain*



# The Regulatory Principles of Glycolysis in Erythrocytes *in vivo* and *in vitro*

## A MINIMAL COMPREHENSIVE MODEL DESCRIBING STEADY STATES, QUASI-STEADY STATES AND TIME-DEPENDENT PROCESSES

By TOM A. RAPOPORT
*Akademie der Wissenschaften der DDR, Zentralinstitut für Molekularbiologie, Berlin-Buch, German Democratic Republic*

and REINHART HEINRICH and SAMUEL M. RAPOPORT
*Humboldt-Universität, Institut für Physiologische und Biologische Chemie, Berlin, German Democratic Republic*

(*Received* 18 *April* 1975)

A simple mathematical model for glycolysis in erythrocytes is presented which takes into account ATP synthesis and consumption. The system is described by four ordinary differential equations. Conditions *in vivo* are described by a stable steady state. The model predicts correctly the metabolite concentrations found *in vivo*. The parameters involved are in agreement with data on the separate steps. The metabolite changes found in pyruvate kinase-deficient erythrocytes and the species variations among erythrocytes from different animals are described satisfactorily. The roles of the enzymes in the control of metabolites and glycolytic flux are expressed in the form of a control matrix and control strengths [R. Heinrich & T. A. Rapoport (1974) *Eur. J. Biochem.* **42**, 89–95] respectively. Erythrocytes from various species are shown to be adapted to a maximal ATP-consumption rate. The calculated eigenvalues reveal the pronounced time-hierarchy of the glycolytic reactions. Owing to the slowness of the 2,3-bisphosphoglycerate phosphatase reaction, quasi-steady states occur during the time-interval of about 0.5–2h incubation, which are defined by perturbed 2,3-bisphosphoglycerate concentrations. The theoretical predictions agree with experimental data. In the quasi-steady state the flux control is exerted almost entirely by the hexokinase–phosphofructokinase system. The model describes satisfactorily the time-dependent changes after addition of glucose to starved erythrocytes. The theoretical consequences are discussed of the conditions *in vitro* with lactate accumulation and the existence of a time-independent conservation quantity for the oxidized metabolites. Even in this closed system quasi-steady states occur which are characterized by approximately constant concentrations of all glycolytic metabolites except for the accumulation of lactate, fructose 1,6-bisphosphate and triose phosphate. The conservation quantity influences both the quasi-steady-state concentrations and the relaxation time of the system. The analysis reveals the main principles for the regulation of ATP concentration. This is kept constant in the cell by three mechanisms. First, the 2,3-bisphosphoglycerate by-pass acts as an 'energy buffer' so that a change in the ATP consumption is compensated for by a variation in the ATP utilization via the by-pass. Secondly, the metabolite 2,3-bisphosphoglycerate acts as an energy source, as it may yield ATP for a certain period at the pyruvate kinase step in case of ATP overconsumption. A third mechanism is observed *in vitro* where ATP changes can be buffered by variations in the accumulation rate of fructose 1,6-bisphosphate and triose phosphate.

In a previous paper a model of glycolysis in erythrocytes in a steady state was described (Rapoport *et al.*, 1974). Glycolysis in erythrocytes was chosen for the model since (1) it is uncontaminated by other interfering pathways, (2) no intracellular compartments exist and (3) all enzyme concentrations are practically constant. The model was essentially linear because the synthesis and breakdown of ATP were disregarded; instead ATP was considered to be a given outer parameter of the system. The model was not applicable to time-dependent processes.

The present model extends the previous one by explicit inclusion of synthesis and breakdown of

ATP in a manner similar to the simplified system of Sel'kov (1975). This was done although many experimental uncertainties about the ATP-consuming processes exist. It is hoped that the interesting theoretical results of the present paper will stimulate further experiments in this direction. A second goal of the investigation was the detailed analysis of the differences between the conditions *in vivo* and *in vitro*. Both steady-state and time-dependent processes were analysed.

The model presented here is still relatively simple, so that it can be used by experimenters directly, the only requirement being a programmable desk calculator. The simplicity of the model is a result of the application of two principles of model reduction. First, there exists a time-hierarchy in metabolic systems (Higgins, 1965; Park, 1974). Some variables are so slow that they remain approximately constant during a specified time-period, and others are so fast that they are in a steady state. Thus only a few essential variables need to be considered. Secondly, parameter reduction is possible since the rate laws of the constituent enzymes essential for the metabolism need not include the details of the enzyme mechanism. Despite the simplicity of the model, which allows the elucidation of some important regulatory features, it describes a multitude of experimental data.

**Symbols and Abbreviations**

*Substrates and metabolites*

Glc-6-*P*, glucose 6-phosphate; Fru-6-*P*, fructose 6-phosphate; Fru-1,6-$P_2$, fructose 1,6-bisphosphate; Gra-3-*P*, glyceraldehyde 3-phosphate; Grn-3-*P*, dihydroxyacetone phosphate; triose-*P*, triose phosphate (sum of Gra-3-*P* and Grn-3-*P*); Gri-1,3-$P_2$, 1,3-bisphosphoglycerate; Gri-3-*P*, 3-phosphoglycerate; Gri-2-*P*, 2-phosphoglycerate; Prv-*P*, phosphoenolpyruvate; Pyr, pyruvate; Lac, lactate; Gri-2,3-$P_2$, 2,3-bisphosphoglycerate.

*Enzymes*

HK, hexokinase (ATP–D-hexose 6-phosphotransferase, EC 2.7.1.1); PGI, phosphoglucoisomerase (D-glucose 6-phosphate ketol-isomerase, EC 5.3.1.9); PFK, phosphofructokinase (ATP–D-fructose 6-phosphate 1-phosphotransferase, EC 2.7.1.11); Ald, aldolase (D-fructose 1,6-bisphosphate D-glyceraldehyde 3-phosphate-lyase, EC 4.1.2.13); TIM, triose phosphate isomerase (D-glyceraldehyde 3-phosphate ketol-isomerase, EC 5.3.1.1); Gra-*P*D, glyceraldehyde phosphate dehydrogenase (D-glyceraldehyde 3-phosphate–$NAD^+$ oxidoreductase, EC 1.2.1.12); Gri-*P*K, phosphoglycerate kinase (ATP–3-phospho-

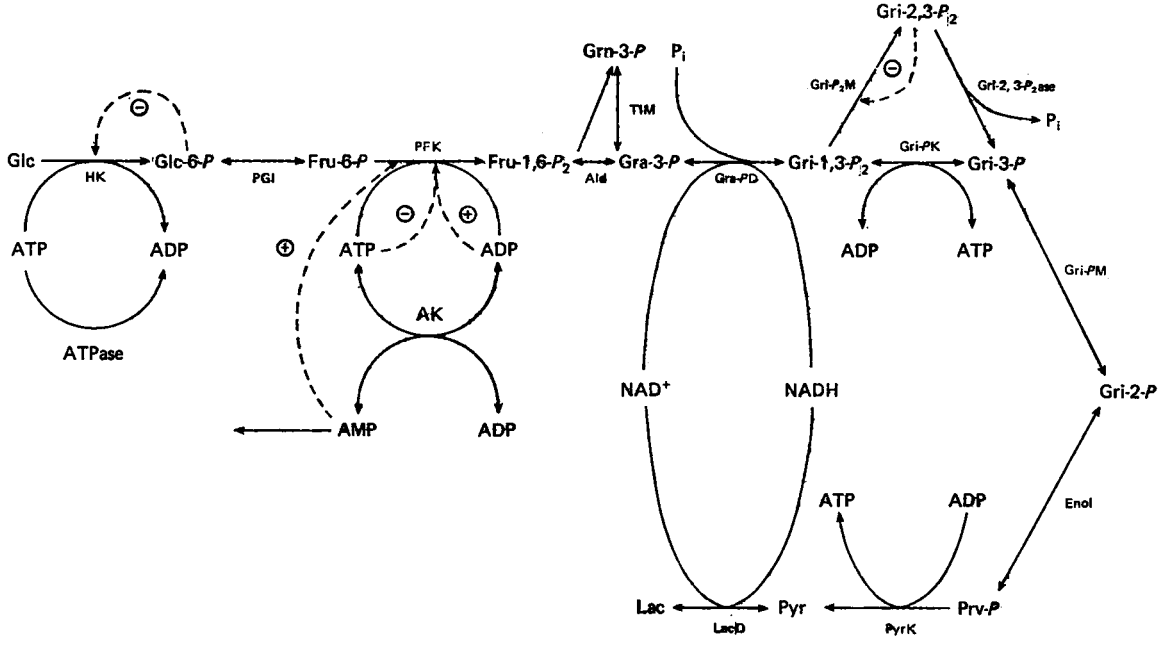


Fig. 1. *Scheme for glycolysis in erythrocytes considered for the model*

All reactions with arrows in both directions were considered to be near to equilibrium. Reactions indicated by an arrow in one direction were considered to be practically irreversible. The broken lines indicate activations (+) or inhibitions (–) of enzymes by metabolites, which were taken into account for the model.

D-glycerate 1-phosphotransferase, EC 2.7.2.3); Gri-PM, phosphoglyceromutase (2,3-bisphospho-D-glycerate–2-phospho-D-glycerate phosphotransferase, EC 2.7.5.3); Enol, enolase (2-phospho-D-glycerate hydrolyase, EC 4.2.1.11); PyrK, pyruvate kinase (ATP–pyruvate phosphotransferase, EC 2.7.1.40); LacD, lactate dehydrogenase (EC 1.1.1.27); Gri-$P_2$M, bisphosphoglycerate mutase (1,3-bisphospho-D-glycerate–2-phospho-D-glycerate phosphotransferase, EC 2.7.5.4); Gri-2,3-$P_2$ase, 2,3-bisphosphoglycerate phosphatase (2,3-bisphospho-D-glycerate 2-phosphohydrolase, EC 3.1.3.13); AK, adenylate kinase (ATP–AMP phosphotransferase, EC 2.7.4.3); ATPase, ATP phosphohydrolase (EC 3.6.1.3).

## Specification of the Model

Fig. 1 shows the scheme for the glycolytic model. It includes both the ATP-producing reactions catalysed by phosphoglycerate kinase and pyruvate kinase and the ATP-consuming reactions catalysed by hexokinase, phosphofructokinase and ATPases. Since there are several enzymes in erythrocytes which degrade ATP (Nakao, 1974), the term 'ATPase' refers not only to the $(Na^+ + K^+)$-dependent ATPase but to the sum of all ATP-consuming reactions. The system includes, further, the $NAD^+$–NADH-dependent reactions of glyceraldehyde phosphate dehydrogenase and lactate dehydrogenase. It takes into account several actions of metabolites as effectors of enzymes: the inhibition by glucose 6-phosphate of hexokinase, the inhibition by ATP and the activation by AMP and ADP of phosphofructokinase and the inhibition by 2,3-bisphosphoglycerate of bisphosphoglycerate mutase. A characteristic feature of glycolysis in erythrocytes is the 2,3-bisphosphoglycerate by-pass (Rapoport & Luebering, 1950, 1951).

The following assumptions were made for the model [for justification see Rapoport *et al.* (1974)].

(*a*) One group of enzymes is considered to catalyse very fast reactions, so that an approximate equilibrium between the reaction partners is maintained under all conditions. This group of enzymes includes phosphoglucoisomerase, aldolase, triose phosphate isomerase, glyceraldehyde phosphate dehydrogenase, phosphoglycerate mutase, enolase, lactate dehydrogenase and adenylate kinase. The following equilibrium relations hold where $q$ is the equilibrium constant:

$$\left.\begin{aligned} q_{PGI} &= \frac{[\text{Fru-6-}P]}{[\text{Glc-6-}P]}, \quad q_{Ald} = \frac{[\text{Gra-3-}P]}{[\text{Fru-1,6-}P_2]}, \\ q_{TIM} &= \frac{[\text{Gra-3-}P]}{[\text{Grn-3-}P]} \\ [P_i]\, q_{Gra\text{-}PD} &\equiv q'_{Gra\text{-}PD} = \frac{[\text{Gri-1,3-}P_2][NADH]}{[\text{Gra-3-}P][NAD^+]}, \\ q_{Gri\text{-}PK} &= \frac{[\text{Gri-3-}P][ATP]}{[\text{Gri-1,3-}P_2][ADP]}, \\ q_{Gri\text{-}PM} &= \frac{[\text{Gri-2-}P]}{[\text{Gri-3-}P]}, \quad q_{Enol} = \frac{[\text{Prv-}P]}{[\text{Gri-2-}P]}, \\ q_{LacD} &= \frac{[Lac][NAD^+]}{[Pyr][NADH]}, \quad q_{AK} = \frac{[ADP]^2}{[ATP][AMP]} \end{aligned}\right\} \quad (1)$$

A fixed ratio of the concentrations of fructose 1,6-bisphosphate and triose phosphate was assumed in accord with experimental data. Actually, the equilibrium assumption for the reactions catalysed by aldolase and triose phosphate isomerase should lead to a quadratic relation (Rapoport *et al.*, 1974).

(*b*) The other enzymes are considered to catalyse practically irreversible reactions: hexokinase, phosphofructokinase, pyruvate kinase, bisphosphoglycerate mutase, 2,3-bisphosphoglycerate phosphatase and ATPase. These enzymes are described by kinetic equations (Table 1). In most cases descriptive rate laws were used which lack a mechanistic basis.

(*c*) The reactions of the hexokinase and phosphofructokinase are lumped into one subsystem with a single response to the adenine nucleotides (Rapoport

Table 1. *Rate laws assumed for the various enzymic steps of the model*

| Enzyme | Rate law | Parameters |
|---|---|---|
| Hexokinase–phosphofructokinase system | $v_{HK-PFK} = \frac{V_{max.}[ATP]}{K_m + [ATP]}$ | $V_{max.}$, maximal velocity<br>$K_m$, half-saturation constant |
| Pyruvate kinase | $v_{PyrK} = k_{PyrK}[ADP][\text{Prv-}P]$ | $k_{PyrK}$, second-order rate constant |
| Bisphosphoglycerate mutase | $v_{Gri\text{-}P_2M} = \frac{k_{Gri\text{-}P_2M}[\text{Gri-1,3-}P_2]}{1+\left(\frac{[\text{Gri-2,3-}P_2]}{K_{Gri\text{-}2,3\text{-}P_2}}\right)}$ | $k_{Gri\text{-}P_2M}$, first-order rate constant<br>$K_{Gri\text{-}2,3\text{-}P_2}$, inhibition constant |
| 2,3-Bisphosphoglycerate phosphatase | $v_{Gri\text{-}2,3\text{-}P_2ase} = k_{Gri\text{-}2,3\text{-}P_2ase}[\text{Gri-2,3-}P_2] + C$ | $k_{Gri\text{-}2,3\text{-}P_2ase}$, first-order rate constant<br>C, zero-order rate constant |
| ATPase | $v_{ATPase} = k_{ATPase}[ATP]$ | $k_{ATPase}$, first-order rate constant |

*et al.*, 1974). It is assumed that glucose 6-phosphate and fructose 6-phosphate are always in a steady state. This approximation is justified, since the relaxation time of phosphofructokinase is relatively short (Table 8). The descriptive rate law given in Table 1 is the result of (1) the action of ATP as the substrate of hexokinase, (2) the activating influence of AMP and ADP and the inhibiting effect of ATP on phosphofructokinase, and (3) the inhibition by glucose 6-phosphate of the hexokinase. A detailed explanation of the rate law is given under 'Fitting of the '*in vivo*' model to experimental data'.

(*d*) For 2,3-bisphosphoglycerate phosphatase two terms are assumed, one proportional to the concentration of its substrate 2,3-bisphosphoglycerate and one independent of it. This assumption is based on the fact that there are several enzymes which degrade 2,3-bisphosphoglycerate (Harkness *et al.*, 1970; Rosa *et al.*, 1975), one of which, the actual 2,3-bisphosphoglycerate phosphatase, probably works at its $V_{max.}$ (denoted by the term C in Table 1). This assumption is valid down to 2,3-bisphosphoglycerate concentrations of about 1 mM (Rose & Liebowitz, 1970).

(*e*) Complex formation of some metabolites with $Mg^{2+}$ and the binding of anions to haemoglobin was neglected. Both effects have a slight but significant influence on metabolite concentrations (Gerber *et al.*, 1973; J. Rapoport, H. Berger, G. Gerber, R. Elsner & S. Rapoport, unpublished work).

(*f*) Two conservation quantities are taken into account: the sum of nicotinamide nucleotides and that of the adenine nucleotides:

$$N = [NAD^+] + [NADH] \quad (2)$$

$$A = [AMP] + [ADP] + [ATP] \quad (3)$$

It is assumed that the processes changing these sums are slow compared with all other reactions included in the model.

(*g*) $P_i$ is taken as an outer parameter which is controlled by the experimenter.

(*h*) Glucose is assumed to be saturating for hexokinase.

These assumptions are supported by experimental data, except for the non-glycolytic ATP-consuming processes, which are poorly characterized.

The time-dependent changes in the concentrations of the metabolites are described by a set of ordinary differential equations. By consideration of the fluxes, $v$, which produce and remove the metabolites, and taking into account the equilibria (1) one obtains the following equations:

$$\frac{d}{dt}(2[\text{Fru-1,6-}P_2] + [\text{triose-}P] + [\text{Gri-1,3-}P_2] + [\text{Gri-3-}P] + [\text{Gri-2-}P] + [\text{Prv-}P]) = 2v_{\text{HK-PFK}} - v_{\text{Gri-}P_2\text{M}} + v_{\text{Gri-2,3-}P_2\text{ase}} - v_{\text{PyrK}} \quad (4)$$

$$\frac{d}{dt}([\text{ATP}] - [\text{AMP}] - [\text{Gri-3-}P] - [\text{Gri-2-}P] - [\text{Prv-}P]) = -2v_{\text{HK-PFK}} - v_{\text{Gri-2,3-}P_2\text{ase}} + 2v_{\text{PyrK}} - v_{\text{ATPase}} \quad (5)$$

$$\frac{d[\text{Gri-2,3-}P_2]}{dt} = v_{\text{Gri-}P_2\text{M}} - v_{\text{Gri-2,3-}P_2\text{ase}} \quad (6)$$

$$\frac{d([\text{Pyr}] + [\text{Lac}])}{dt} = v_{\text{PyrK}} + v_{\text{exchange}} \quad (7)$$

Eqn. (5) is the result of three differential equations:

$$\frac{d[\text{ATP}]}{dt} = -2v_{\text{HK-PFK}} + v_{\text{PyrK}} + v^+_{\text{Gri-PK}} - v^-_{\text{Gri-PK}} + v^+_{\text{AK}} - v^-_{\text{AK}} - v_{\text{ATPase}}$$

$$\frac{d[\text{AMP}]}{dt} = v^+_{\text{AK}} - v^-_{\text{AK}}$$

$$\frac{d}{dt}([\text{Gri-3-}P] + [\text{Gri-2-}P] + [\text{Prv-}P]) = v^+_{\text{Gri-PK}} - v^-_{\text{Gri-PK}} + v_{\text{Gri-2,3-}P_2\text{ase}} - v_{\text{PyrK}}$$

where the + and − signs indicate the forward and backward reactions respectively. From these three differential equations the slow motion is extracted, described by eqn. (5) (Tichonov, 1948; Park, 1974).

When the kinetic equations of Table 1 are introduced, the right-hand sides of eqns. (4)–(7) become functions of the metabolite concentrations and the parameters of the enzymes. The differential equations are non-linear. The metabolite concentrations are determined not only by differential eqns. (4)–(7) but also by the equilibrium relations (1) and by the conservation eqns. (2) and (3).

## The System of Glycolysis *in vivo*

### *The steady states*

*Steady-state equations and general features of the solutions.* The steady-state solutions for the metabolites can be obtained by setting the time-derivatives on the left side of the differential eqns. (4)–(7) equal to zero. The steady-state concentrations of pyruvate and lactate can be calculated from eqn. (7) and depend on the term $v_{\text{exchange}}$ which is determined by other tissues of the body. Owing to the equilibria at glyceraldehyde phosphate dehydrogenase and lactate dehydrogenase, the concentrations of fructose 1,6-bisphosphate and triose phosphate depend also on processes outside the erythrocytes. On the other hand, since the concentrations of pyruvate and lactate do not appear in eqns. (4)–(6) they do not influence the steady-state concentrations of the other glycolytic metabolites. One may therefore call the metabolic system described by eqns. (4)–(6) the 'core' of glycolysis. It is essentially the energy metabolism of this pathway.

The steady-state equations now have the following form:

$$\frac{2V_{max.}[ATP]}{K_m+[ATP]}-\frac{k_{Gri\text{-}P_2M}[Gri\text{-}1,3\text{-}P_2]}{1+\left(\frac{[Gri\text{-}2,3\text{-}P_2]}{K_{Gri\text{-}2,3\text{-}P_2}}\right)}+k_{Gri\text{-}2,3\text{-}P_2ase}[Gri\text{-}2,3\text{-}P_2]+C-k_{PyrK}[ADP][Prv\text{-}P]=0 \quad (8)$$

$$\frac{k_{Gri\text{-}P_2M}[Gri\text{-}1,3\text{-}P_2]}{1+\left(\frac{[Gri\text{-}1,3\text{-}P_2]}{K_{Gri\text{-}2,3\text{-}P_2}}\right)}-k_{Gri\text{-}2,3\text{-}P_2ase}[Gri\text{-}2,3\text{-}P_2]-C=0 \quad (9)$$

$$-\frac{2V_{max.}[ATP]}{K_m+[ATP]}-k_{Gri\text{-}2,3\text{-}P_2ase}[Gri\text{-}2,3\text{-}P_2]-C+2k_{PyrK}[ADP][Prv\text{-}P]-k_{ATPase}[ATP]=0 \quad (10)$$

In these equations the variables are ATP, ADP, 1,3-bisphosphoglycerate, 2,3-bisphosphoglycerate and phosphoenolpyruvate. By use of the equilibria (1), phosphoenolpyruvate can be expressed by 1,3-bisphosphoglycerate, ATP and ADP. Further, 2,3-bisphosphoglycerate and 1,3-bisphosphoglycerate can be eliminated from eqns. (8)–(10), yielding an equation for ATP and ADP:

$$\left[\frac{2V_{max.}[ATP]}{K_m+[ATP]}-\frac{(q_{Enol}q_{Gri\text{-}PM}q_{Gri\text{-}PK})k_{PyrK}[ADP]^2}{k_{Gri\text{-}P_2M}[ATP]}\left(\frac{2V_{max.}[ATP]}{K_m+[ATP]}-k_{ATPase}[ATP]\right)\right]\times\left[1+(k_{Gri\text{-}2,3\text{-}P_2ase}K_{Gri\text{-}2,3\text{-}P_2})^{-1}\left(\frac{2V_{max.}[ATP]}{K_m+[ATP]}-k_{ATPase}[ATP]-C\right)\right]=0 \quad (11)$$

Finally, ADP can be expressed as a function of ATP by using the conservation quantity for the adenine nucleotides and the equilibrium of adenylate kinase:

$$[ADP]=\frac{q_{AK}[ATP]}{2}\left[\sqrt{1+\frac{4}{q_{AK}}\left(\frac{A}{[ATP]}-1\right)}-1\right] \quad (12)$$

There are several solutions of eqns. (11) and (12). One with [ATP] = zero is obvious. Dividing eqn. (11) by [ATP], the resulting expression may be transformed into a polynomial in the ATP concentration, the roots of which are further solutions. The degree of the polynomial, however, is rather high. Another procedure is much simpler. The implicit equation for [ATP] is solved for a parameter (Table 1) as a function of the ATP concentration. This yields, for example, for $k_{ATPase}$ and $V_{max.}$ a quadratic, or for $k_{Gri\text{-}P_2M}$ a linear relationship. With their help steady-state lines for the metabolite concentrations can be constructed.

The concentrations of 2,3-bisphosphoglycerate, 1,3-bisphosphoglycerate and phosphoenolpyruvate can be obtained from the solutions for ATP by the following expressions:

$$[Gri\text{-}2,3\text{-}P_2]=\left(\frac{2V_{max.}[ATP]}{K_m+[ATP]}-k_{ATPase}[ATP]-C\right)k^{-1}_{Gri\text{-}2,3\text{-}P_2ase} \quad (13a)$$

$$[Gri\text{-}1,3\text{-}P_2]=(k_{Gri\text{-}2,3\text{-}P_2ase}[Gri\text{-}2,3\text{-}P_2]+C)\left(1+\frac{[Gri\text{-}2,3\text{-}P_2]}{K_{Gri\text{-}2,3\text{-}P_2}}\right)\times k^{-1}_{Gri\text{-}P_2M} \quad (13b)$$

$$[Prv\text{-}P]=q_{Enol}q_{Gri\text{-}PM}q_{Gri\text{-}PK}\left(\frac{[ADP][Gri\text{-}1,3\text{-}P_2]}{[ATP]}\right) \quad (13c)$$

The concentrations of 3-phosphoglycerate and 2-phosphoglycerate are determined by the equilibria for the enolase and phosphoglycerate mutase reactions. The concentrations of fructose 1,6-bisphosphate and triose phosphate can be obtained by the equilibria (1) and eqns. (13a–c) from the given concentrations of pyruvate and lactate.

Typical steady-state curves of the metabolite concentrations are given in Figs. 2 and 3. All curves have common characteristics. The first feature is that there is only a limited range for the parameter values for which steady states exist. Beyond a critical value only the steady state exists corresponding to zero concentrations of ATP, ADP and the phosphoglycerates. There is a sharp change of the steady-state values at the critical point (bifurcation point). One should keep in mind that the time needed for the critical change cannot be inferred from the curves. The steady-state space is limited by the permissible values of both variables and parameters. The reasons are of complex nature. One is the existence of a conservation restriction for the adenine nucleotides which confines their variation. Another reason is the special structure of the energy system. Thus the following flux equation is easily derived from eqns. (8)–(10):

$$v_{Gri\text{-}P_2M}=2v_{HK-PFK}-v_{ATPase} \quad (14)$$

If either $v_{ATPase}$ is increased (by change of $k_{ATPase}$) or $v_{HK-PFK}$ decreased (by change of, e.g. $V_{max.}$) beyond certain limits negative values for the by-pass flux arise, which are, of course, unrealistic. Therefore $k_{ATPase}$ and $V_{max.}$ are limited in their range.

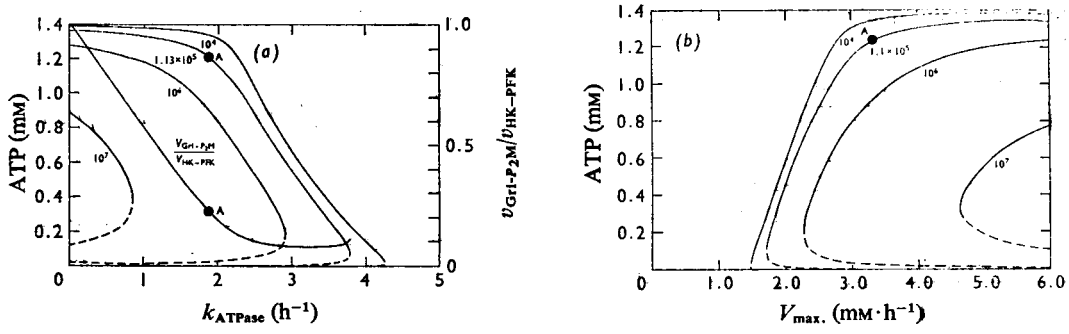


Fig. 2. *ATP concentration and flux through the* 2,3-*bisphosphoglycerate by-pass as functions of the rate constant of the ATPase* ($k_{ATPase}$) (*a*) *and of the hexokinase–phosphofructokinase system* ($V_{max.}$) (*b*)

The parameter of the bisphosphoglycerate mutase ($k_{Gri\text{-}P_2M}$) was varied (numbers in the Figure in $h^{-1}$). The other parameter values are those given in Table 2. Unstable steady states are indicated by broken lines. $v_{Gri\text{-}P_2M}/v_{HK\text{-}PFK}$ gives the share of the total flux which flows through the 2,3-bisphosphoglycerate by-pass. This curve was plotted with $k_{Gri\text{-}P_2M} = 1.1\times10^5 h^{-1}$. The points A indicate the state of the system *in vivo*.

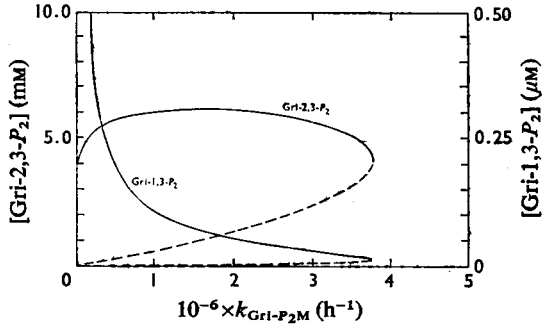


Fig. 3. *Concentrations of* 2,3-*bisphosphoglycerate and* 1,3-*bisphosphoglycerate as functions of the rate constant of bisphosphoglycerate mutase* ($k_{Gri\text{-}P_2M}$)

The curves were calculated with the parameter values given in Table 2. The broken lines indicate unstable steady states.

A second characteristic is the existence of multiple steady states. For a given parameter combination there exist three steady states, one of which is [ATP] = zero. Multiple steady states occur generally in non-linear systems.

The third feature is the occurrence of stable and unstable steady states. 'Stable' means that the system after some arbitrarily small perturbation from the steady state will return to it. The broken lines in Figs. 2 and 3 correspond to unstable steady states. Steady states found *in vivo* must correspond to stable steady states. The stability analysis has been performed by standard methods. The differential equations are linearized in the neighbourhoods of the stationary points and the signs of the eigenvalues have been investigated by application of the Routh–Hurwitz criterion (see e.g., Willems, 1973). The system is stable if the eigenvalues have all negative real parts, otherwise it is unstable. A simple steady-state analysis without investigation of the stability properties may be quite misleading since it might refer to an unstable state which has no correspondence to reality.

2,3-*Bisphosphoglycerate by-pass acting as an energy buffer.* The ATP concentration is influenced in an opposite manner by the ATPase rate constant ($k_{ATPase}$) and by the $V_{max.}$ value of the hexokinase–phosphofructokinase system (Fig. 2); [ATP] decreases with increasing $k_{ATPase}$. However, there is a region in the curves where the ATP concentration is relatively constant. This is brought about by the 2,3-bisphosphoglycerate by-pass, which acts as an 'energy buffer'. If the ATP consumption increases, the share of the flux through the by-pass decreases so that more ATP can be produced at the phosphoglycerate kinase step. At low fluxes through the by-pass an increase in the ATPase constant cannot be compensated for by a decrease in the ATP utilization by the by-pass, and therefore the ATP concentration falls (Fig. 2*a*). Identical effects are produced by a decrease in the $V_{max.}$ value of the hexokinase–phosphofructokinase system. The 2,3-bisphosphoglycerate by-pass may be considered as an example of a futile cycle. It may be suggested that futile cycles in general serve as 'energy buffers' in cells.

*Fitting of the 'in vivo' model to experimental data.* In this section two tests are described: (1) predictive power of the model for the metabolite concentrations, and (2) correspondence of the chosen parameter values to those obtained by independent experimental methods.

The various data sets from different experimental series were analysed with a constant set of parameter values for standard conditions (pH 7.2, 37°C, 1 mM-$P_i$). Owing to systematic errors within a series of experiments and owing to biological variations, the experimental data for standard conditions vary somewhat in the literature. In some cases a better agreement of data and theory might have been found by adjustment of the standard parameters. We have refrained from doing so to avoid the overweighting of a single experiment.

Table 2 contains the parameter values that give the best correspondence between predicted and observed metabolite concentrations in the steady state *in vivo* (in view of the small variation in the volume of erythrocytes under the conditions to be considered, the concentrations are given in mol per litre of cells, instead of per litre of cell water). The values were used for the calculation of all curves except where indicated otherwise. This parameter set gives the point A in Fig. 2 at which the glycolysis in erythrocytes is expected to work *in vivo*.

Since the number of parameters greatly exceeds that of independent variables, the best parameter set is not unique. The combination given in Table 2 was chosen so that the values also agree with data on isolated enzymic steps. Data on purified 2,3-bisphosphoglycerate mutase (Rose, 1968, 1973) and pyruvate kinase (Oski & Bowman, 1969) show good agreement between the values (Table 3; see also Rapoport *et al.*, 1974). For 2,3-bisphosphoglycerate

Table 2. *Comparison of calculated and measured concentrations of the metabolites in vivo by using the best set of parameter values*

The following set of values of the parameters yielded the best agreement with the experimental data: $V_{max.} = 3170\,\mu M \cdot h^{-1}$; $K_m = 1400\,\mu M$; $k_{ATPase} = 1.92\,h^{-1}$, $k_{PyrK} = 0.67\,\mu M^{-1} \cdot h^{-1}$; $k_{Grl\text{-}P_2M} = 1.1 \times 10^5\,h^{-1}$; $k_{Grl\text{-}2,3\text{-}P_2ase} = 0.1\,h^{-1}$; $C = 110\,\mu M \cdot h^{-1}$. For the equilibrium constants $q_{Enol}$ and $q_{Grl\text{-}PM}$ the values 0.18 and 2.8 respectively were used. The value of 600 for $q_{Grl\text{-}PK}$ was chosen on the basis of the equilibrium assumption and of experimentally determined metabolite concentrations. It is in fair agreement with the thermodynamic constant for intracellular conditions (Rose & Warms, 1970). For $K_{Grl\text{-}2,3\text{-}P_2}$ a value of 40 $\mu$M was used in approximate agreement with data given by Rose (1973). For $q_{AK}$ a value of 0.5 was used. The data refer to pH 7.2 and 1 mM-$P_i$.

| Metabolite | Calculated concentration ($\mu$M) | Measured concentration ($\mu$M) |
|---|---|---|
| ATP | 1184 | 1200 |
| ADP | 167 | 185 |
| AMP | 43 | 50 |
| 2,3-Bisphosphoglycerate | 4900 | 4700 |
| 1,3-Bisphosphoglycerate | 0.6 | 0.5 |
| 3-Phosphoglycerate | 52 | 60 |
| 2-Phosphoglycerate | 10 | 15 |
| Phosphoenolpyruvate | 27 | 26 |
| Glycolytic flux ($\mu M \cdot h^{-1}$) | 1480 | 1350 |

Table 3. *Comparison of some parameter values of Table 2 with data on the isolated steps*

The rate constants for pyruvate kinase and bisphosphoglycerate mutase were calculated by assuming simple rate laws (Rapoport *et al.*, 1974). The rate of the 2,3-bisphosphoglycerate phosphatase reaction was measured by incubating erythrocytes in the absence of glucose, i.e. in the absence of 2,3-bisphosphoglycerate formation (Tomoda & Minakami, 1975).

| Quantity | Value obtained by fitting to metabolite concentrations | Value obtained from data on the isolated step |
|---|---|---|
| $k_{PyrK}$ ($\mu M^{-1} \cdot h^{-1}$) | 0.67 | 1.0 |
| $k_{Grl\text{-}P_2M}$ ($h^{-1}$) | $1.1 \times 10^5$ | $5.4 \times 10^4$–$8 \times 10^4$ |
| $v_{Grl\text{-}2,3\text{-}P_2ase}$ ($\mu M \cdot h^{-1}$) | 600 | 600 |

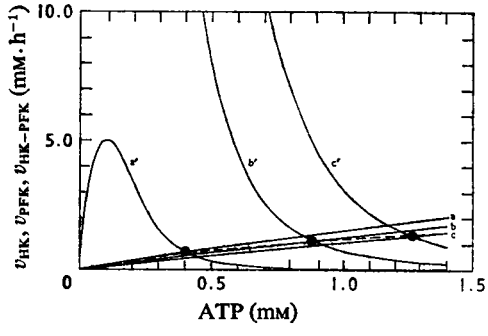


Fig. 4. *Construction of the ATP response of the hexokinase–phosphofructokinase system*

The ATP-dependence of the hexokinase and phosphofructokinase reactions was calculated according to the kinetic models proposed for them [Gerber *et al.* (1974) and Otto *et al.* (1974) respectively]. The parameter values were transformed into values per litre of cells. A maximal activity of 200 $\mu M \cdot h^{-1}$ for the phosphofructokinase was used (Jacobasch *et al.*, 1974). Complex-formation of ATP with $Mg^{2+}$, the action of $Mg^{2+}$ on the enzymes and the binding of 2,3-bisphosphoglycerate to haemoglobin were taken into account. The net flux through the system is given by the intersection points of the curves for specified concentrations of glucose 6-phosphate and fructose 6-phosphate. The broken curve was calculated according to the rate law for the system given in Table 1. a, b, c, Hexokinase flux; a', b', c', phosphofructokinase flux; a, a', [glucose 6-phosphate] = 5 $\mu$M; b, b', [glucose 6-phosphate] = 50 $\mu$M; c, c', [glucose 6-phosphate] = 100 $\mu$M. The concentration of fructose 6-phosphate was obtained from the equilibrium for phosphoglucoisomerase (0.41).

phosphatase the overall rate can be measured separately from other interfering reactions. The data on the isolated reaction compare well with the values *in vivo* (Table 3). No data are available for ATPase. The ATP response of the hexokinase–phosphofructokinase system was constructed on the basis of the kinetic models for hexokinase (Gerber *et al.*, 1974) and phosphofructokinase (Otto *et al.*, 1974). Fig. 4 shows that despite the strong ATP response of both enzymes, the net flux of the system (points in Fig. 4) shows little dependence on the ATP concentration. The net flux can be satisfactorily approximated by the rate law given in Table 2 (broken line in Fig. 4). Since the inhibition by glucose 6-phosphate of the hexokinase in the kinetic model is rather weak, the strong inhibition by ATP of the phosphofructokinase cannot have a great influence on the total flux. There is, however, some doubt about the strength of the inhibition by glucose 6-phosphate arising both from studies on the isolated enzyme (Kosow *et al.*, 1973) and on intact cells (Rose & O'Connell, 1964; Jacobasch *et al.*, 1974). A stronger influence of glucose 6-phosphate would lead to a flatter curve in Fig. 4, but one would not expect an overall inhibition by ATP. The calculation of the curves in Fig. 4 is based on preliminary studies by T. Geyer & M. Glende (unpublished work).

*Control properties of the steady states in vivo.* This section contains the analysis of the influence of the enzymes on metabolites and flux as well as experimental tests of the derivations.

Control of the concentrations of the metabolites. The influence of the activity $v_j$ of an enzyme $E_j$ on the metabolite concentration $S_i$ can be expressed by an element of the control matrix $S_{ij}$ (Heinrich & Rapoport, 1974):

$$S_{ij} = \frac{\delta \ln S_i}{\delta \ln v_j} \qquad (15)$$

A positive value indicates that activation of the enzyme leads to an increase in the concentration of the metabolite, and a negative value has the opposite meaning. Rules for the calculation of the control matrix, which are also applicable for non-linear steady-state systems, have been derived by Heinrich & Rapoport (1975).

In Table 4 some calculated elements of the control matrix at the '*in vivo* point' are given. The elements of the control matrix for the remaining metabolites can be easily calculated from those given in Table 4. For equilibrium enzymes the elements are zero. The following qualitative conclusions can be drawn from the data of Table 4.

The ATP concentration is mainly determined by the hexokinase–phosphofructokinase system and by the ATP-consuming processes. Other enzymes have little influence on the ATP concentration. The 2,3-bisphosphoglycerate concentration is mainly controlled by the same enzymes. Additionally, 2,3-bisphosphoglycerate phosphatase has a significant influence, whereas bisphosphoglycerate mutase has only little effect. This is explained as follows. The flux through the by-pass is determined by eqn. (14) so that it is a strict function of the ATP concentration. The bisphosphoglycerate mutase has an insignificant influence on the ATP concentration, so that its variation will not produce great changes in the flux through the by-pass. Consequently, the 2,3-bisphosphoglycerate concentration will also be little affected. Any change in the rate constant of the bisphosphoglycerate mutase is counterbalanced by a corresponding inverse change in the 1,3-bisphosphoglycerate concentration (see Fig. 3). This example demonstrates that the whole system must be analysed rather than parts or even single steps. The phosphoenolpyruvate concentration is influenced by all enzymes, especially by the hexokinase–phosphofructokinase system and by the ATPases.

Table 4. *Control matrix at the 'in vivo point'*

The elements of the matrix give the relative dependence of the metabolite concentrations on the enzyme activities (see eqn. 15). For each metabolite the sum of the elements of the control matrix must be zero.

| Enzyme | ATP | 2,3-Bisphosphoglycerate | Phosphoenolpyruvate |
|---|---|---|---|
| Hexokinase–phosphofructokinase system | 0.80 | 4.88 | 4.70 |
| ATPase | −0.70 | −3.83 | −3.22 |
| Pyruvate kinase | 0.10 | −0.10 | −0.63 |
| Bisphosphoglycerate mutase | −0.10 | 0.10 | −0.42 |
| 2,3-Bisphosphoglycerate phosphatase | −0.10 | −1.05 | −0.43 |

Flux control. The control strength $C_i$ has been defined as a measure of the influence of an enzyme on the overall flux in the following way (Heinrich & Rapoport, 1974):

$$C_i = \frac{\delta \ln v_g}{\delta \ln v_i} \qquad (16)$$

$v_g$ denotes the total flux and $v_i$ the flux through the enzyme $E_i$. The control strengths of the glycolytic enzymes were computed as functions of the parameter $k_{ATPase}$. Several interesting features are revealed. With increasing $k_{ATPase}$ values all control strengths increase in their absolute values and reach infinity at the bifurcation point. The hexokinase–phosphofructokinase system, which is favoured for flux control by its position in the glycolytic chain (Heinrich & Rapoport, 1974), has a control strength greater than unity even at low $k_{ATPase}$ values. Activation of the hexokinase–phosphofructokinase

Table 5. *Comparison of the control strengths for the model in vivo and the previous model (Rapoport et al., 1974)*

The definition of the control strength is given in eqn. (16). In the previous model hexokinase and phosphofructokinase were considered separately.

| Enzyme | Control strength: Model *in vivo* | Control strength: Previous model |
|---|---|---|
| Hexokinase–phosphofructokinase system | 1.37 | 0.69* 0.31† |
| ATPase | –0.33 | — |
| Pyruvate kinase | 0.04 | 0 |
| Bisphosphoglycerate mutase | –0.04 | 0 |
| 2,3-Bisphosphoglycerate phosphatase | –0.04 | 0 |

* Control strength of hexokinase.
† Control strength of phosphofructokinase.

system leads to an increase in [ATP] so that its control strength is higher than it would be without feedback. ATPase, 2,3-bisphosphoglycerate phosphatase and bisphosphoglycerate mutase have negative control strengths. Activation of these enzymes leads to a decrease in the overall flux caused by a diminished ATP concentration (see Table 4). The enzymes of the by-pass have small control strengths owing to their small element in the control matrix. Pyruvate kinase has a small positive control strength. In the range of $k_{ATPase}$ values where ATP falls, its concentration becomes more sensitive to parameter changes and the control strengths of all enzymes increase. The numerical values for the control strengths calculated for the '*in vivo* point' are compared in Table 5 with the values yielded by the simpler model (Rapoport *et al.*, 1974). Obviously, the main conclusion is identical: the hexokinase–phosphofructokinase system has the most pronounced influence on the flux. The inclusion of the ATPases results in some differences with respect to the regulation of the metabolites. In the simpler model the bisphosphoglycerate mutase and the 2,3-bisphosphoglycerate phosphatase influenced the 2,3-bisphosphoglycerate concentration only. In the extended model the bisphosphoglycerate mutase has less control of the 2,3-bisphosphoglycerate concentration, whereas additional metabolites, in particular phosphoenolpyruvate, are influenced. The hexokinase–phosphofructokinase system has a much greater effect on the 2,3-bisphosphoglycerate and phosphoenolpyruvate concentrations than calculated before (Rapoport *et al.*, 1974). Under 'Control properties of the quasi-steady state at perturbed 2,3-bisphosphoglycerate concentrations' it will be shown that the previous model corresponds better to that of a quasi-steady state.

Experimental tests of the influence of the parameters on the metabolite concentrations and flux. The test of the predicted influence of the parameters on the metabolites requires experimental transitions from one steady state to another. A good test is provided by enzyme deficiencies, and pyruvate kinase deficiency will be considered as an example. The case cited in Table 6 (Jacobasch *et al.*, 1969) was chosen because of its low reticulocytosis so that all effects may be ascribed to the erythrocytes. The maximal velocity of the pyruvate kinase was diminished to about one-tenth, whereas the maximal velocities of the other enzymes remained unchanged. Insertion of the low constant of the pyruvate kinase into the standard set of parameters yielded the predicted metabolite concentrations and the flux given in Table 6. They are in reasonable agreement with the experimental data.

Another kind of validation of the model is provided by a comparison of data on different animal species. Of course, many factors such as differences in the properties of the enzymes and of the internal milieu of the cells had to be neglected. Nevertheless, it seemed interesting to find out whether the model can explain qualitatively the species variations observed. Table 7 gives relevant data for man, rat, rabbit and goat (Jacobasch, 1970). The values for the total adenine nucleotides were then sufficient to predict the 2,3-bisphosphoglycerate concentration. For the prediction of the flux the value $K_m/A$ was held at unity for all species. The correspondence between data and theory supports this assumption. Table 7 shows that the 2,3-bisphosphoglycerate concentration was predicted reasonably well for all species except for the goat. Here a discrepancy of an order of magnitude remained which may be due to uncertainties in the estimates of the maximal velocities for the enzymes of the by-pass. The discrepancies in the ATP concentration are due to the fact that the error calculated for human erythrocytes is propagated for all other species.

Table 6. *Prediction of some metabolite concentrations and the flux for a case of hereditary pyruvate kinase deficiency*

The maximal velocity of the pyruvate kinase in the erythrocyte of the patient C. S. was diminished to 26 mM·h$^{-1}$ (normal value 235 mM·h$^{-1}$). Reticulocytosis was less than 8% (Jacobasch *et al.*, 1969).

| Metabolite | Theoretically predicted (μM) | Experimentally observed (μM) |
|---|---|---|
| ATP | 870 | 940 |
| Phosphoenolpyruvate | 106 | 144 |
| 2,3-Bisphosphoglycerate | 6300 | 6100 |
| Glycolytic flux (μM·h$^{-1}$) | 1200 | 1600 |

Table 7. *Prediction of the concentration of 2,3-bisphosphoglycerate and the glycolytic flux for erythrocytes of various animal species*

The data in the legend to Fig. 5 were used to predict the concentrations of 2,3-bisphosphoglycerate and the glycolytic flux for the various species. The ATP concentration in erythrocytes of man was theoretically predicted, those of the other species were calculated by assuming 85% of the adenine nucleotides to be ATP. The flux was determined at pH8.2.

| | ATP ($\mu$M) | | 2,3-Bisphosphoglycerate ($\mu$M) | | Flux ($\Delta$[lactate], mM·h$^{-1}$) | |
|---|---|---|---|---|---|---|
| Species | Theoretical | Experimental | Theoretical | Experimental | Theoretical | Experimental |
| Man | 1180 | 1500 | 4.9 | 4.5 | 4.2* | 4.2 |
| Rat | 870 | 1100 | 5.3 | 5.5 | 8.4 | 10.3 |
| Rabbit | 1600 | 2000 | 6.3 | 7.2 | 5.9 | 7.4 |
| Goat | 390 | 500 | 0.5 | 0.03 | 1.3 | 2.0 |

* The theoretical value was adjusted in the case of man to the experimental value ($V_{max.}$ adjusted).

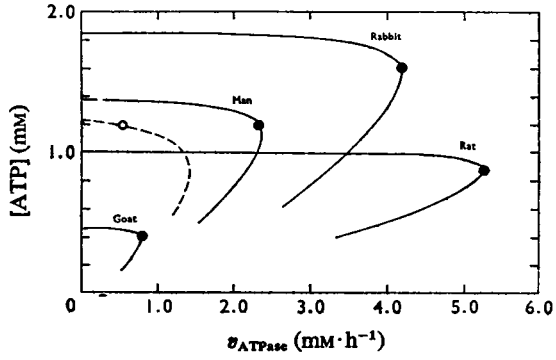


Fig. 5. *ATP concentration as a function of the rate of the non-glycolytic ATP-consuming processes ($v_{ATPase}$) for erythrocytes from various species*

The rate of the ATPase is given by $v_{ATPase} = k_{ATPase}$[ATP]. The parameter values for the erythrocytes from man are given in Table 2, those for the other species are as follows (given in the order rat, rabbit, goat; Jacobasch, 1970): $V_{max.} = 6340$, 4440, 950 $\mu$M·h$^{-1}$; $k_{PyrK} = 0.36$, 1.04, 0.33 $\mu$M$^{-1}$·h$^{-1}$; $k_{Grl\text{-}P_2M} = 4.95\times10^4$, $1.4\times10^5$, $3.85\times10^3$ h$^{-1}$; $k_{Grl\text{-}2,3\text{-}P_2ase} = 0.04$, 0.087, 0.047 h$^{-1}$; C = 45, 96, 52 $\mu$M·h$^{-1}$; A = 1020, 1870, 462 $\mu$M; $K_m$ = 1020, 1870, 462 $\mu$M. All other parameters have the same values as given in Table 2. It was assumed that in all cells 85% of the total adenine nucleotides are present as ATP. The points give the '*in vivo* points' for the cells. The broken line gives a simulated situation where the parameter $k_{Grl\text{-}P_2M}$ had a value of $1.1\times10^6$ h$^{-1}$, but all other values are identical with those given in Table 2.

*Optimum location of the 'in vivo point'.* Fig. 5 gives plots of the ATP concentration versus the rate of the ATP-consuming processes (i.e. $k_{ATPase}\times$[ATP]) for erythrocytes of various species. All curves display a maximum with respect to the ATPase rate. This can be explained as follows. At high ATP concentrations an increase in $k_{ATPase}$, which means an increase in $v_{ATPase}$, will cause small changes in the ATP concentration owing to the compensation by the 2,3-bisphosphoglycerate by-pass (see under '2,3-Bisphosphoglycerate by-pass acting as an energy buffer'). If the share of the by-pass has reached low values the decrease in the ATP concentration results in a decreased ATP synthesis, and therefore the rate of the ATPase must also decrease. Fig. 5 shows that in all species the '*in vivo* point' is located at the maximum. This is especially surprising as the various rate constants among the species differ by more than one order of magnitude. A similar but arbitrarily chosen change in the rate constants of bisphosphoglycerate mutase can lead to quite a different position of the steady-state point (open circle in Fig. 5). Thus the location of the '*in vivo* point' does not seem to be fortuitous but rather the result of an evolutionary adaption. The cells of the various species differ with respect to the absolute work they can do, but they all perform at maximal efficiency, i.e. they do maximal work at minimal glucose consumption.

The '*in vivo* point' appears to represent a compromise between a high ATP concentration, i.e. high glycolytic flux and ATP production on the one hand, and on the other a small share of the ATP-wasting 2,3-bisphosphoglycerate by-pass (10–20% of the total glycolytic flux, see Fig. 2*a*).

*Time-hierarchy of the glycolytic system*

For small deviations of the metabolite concentrations, $S_i$, from their steady-state values, $S_i^0$, the dynamics of the system are determined by linear differential equations. The solutions are of the general form:

$$S_i(t) = S_i^0 + \sum_{k=1}^{m} c_k A_i^k e^{\lambda_k t} \qquad (17)$$

where $\lambda_k$ and $A_i^k$ are the eigenvalues and the eigenvectors respectively of the Jacobian of the linearized system. The coefficients $c_k$ depend on the starting conditions of the time-dependent process. The reciprocal real parts of the eigenvalues have the

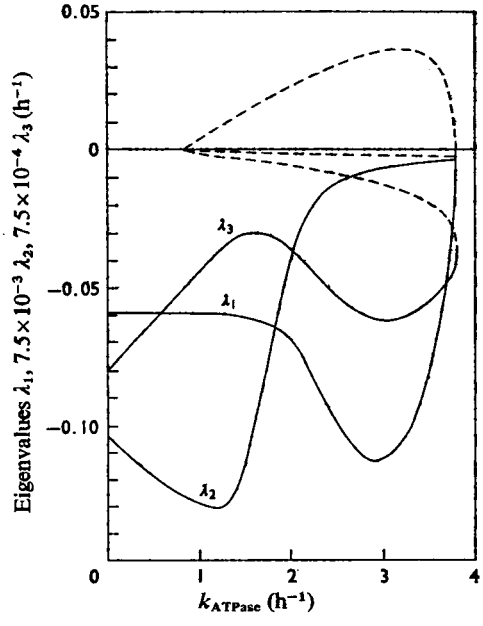


Fig. 6. *Eigenvalues of the glycolytic system* ($\lambda$) *as functions of the rate constant of the ATPase* ($k_{ATPase}$)

The reciprocal eigenvalues characterize the slowness of the relaxation of the system. At the '*in vivo* point' the eigenvalues have the following values: $\lambda_1 = -0.068\,h^{-1}$, $\lambda_2 = -6.6\,h^{-1}$, $\lambda_3 = -45.84\,h^{-1}$.

dimensions of time and characterize the slowness of the relaxation process. The eigenvalues are complex functions of the kinetic parameters of the enzymes so that they usually cannot be attributed to the relaxation of isolated single reactions.

In Fig. 6 the calculated eigenvalues of the '*in vivo*' equation system (4)–(6) are plotted versus $k_{ATPase}$. Numerical values for the '*in vivo* point' are also given in the legend. The eigenvalues are real. At the bifurcation point the smallest eigenvalue changes its sign and is therefore responsible for the existence of the unstable branches in the steady-state curves. The three eigenvalues are of different orders of magnitude. This expresses the fact that the glycolysis in erythrocytes exhibits a pronounced time-hierarchy. The most important feature is the great difference between the two smallest eigenvalues (by a factor of 100 at the '*in vivo* point').

In Table 8 the characteristic times [for definition see Heinrich & Rapoport (1974)] of the glycolytic enzymes are given: they vary over almost four orders of magnitude. This is further proof for the time-hierarchy of the glycolytic system. It is evident that the slowness of the 2,3-bisphosphoglycerate phosphatase is responsible for the slow changes with the relaxation time $-1/\lambda_1$.

Table 8. *Characteristic times of some enzymic steps included in the model*

The characteristic times ($\tau$) were calculated from the rate laws $v(S_i)$. $\tau$ is for a one-substrate reaction $(\delta v/\delta S)^{-1}$ and for a two-substrate reaction $[(\delta v/\delta S_1)+(\delta v/\delta S_2)]^{-1}$.

| Enzyme | Characteristic time ($\tau$) |
|---|---|
| Hexokinase–phosphofructokinase system | 1.5h |
| ATPase | 0.5h |
| Pyruvate kinase | 28s |
| Bisphosphoglycerate mutase | 3.9s |
| 2,3-Bisphosphoglycerate phosphatase | 10h |
| Hexokinase* | 0.6h |
| Phosphofructokinase* | 74s |

* These values were obtained previously (Rapoport *et al.*, 1974) by use of linear rate laws. The characteristic time of the system as a whole is slower than that of any individual enzyme because of the inhibition by glucose 6-phosphate of the hexokinase.

As a consequence of the time-hierarchy of the glycolytic structure, the differential eqns. (4)–(7) are 'stiff'. Numerical integrations of the system are performed as described by Park (1974). The time-derivatives of equations which describe very fast movements of metabolite pools are set equal to zero, i.e. these pools are considered to be in the steady state. Thus only the differential equations describing slow movements remain for the integration, and the other equations serve only as an algebraic subsystem which has to be solved simultaneously. Under conditions *in vivo* eqn. 4 describes a very fast movement of the pool ([Gri-1,3-$P_2$]+[Gri-3-$P$]+[Gri-2-$P$]+[Prv-$P$]). After perturbation of the concentrations of the metabolites it is nearly in the steady state after a few minutes. The quantity ([ATP]−[AMP]−[Gri-3-$P$]−[Gri-2-$P$]−[Prv-$P$]) also approaches the steady state after about 1h. If one considers longer time-periods only the differential eqn. (6) for 2,3-bisphosphoglycerate remains for integration. It was checked that during the integration the fast pools remain in the steady state (Park, 1974). By this procedure the time required for numerical integration of the differential eqns. (4)–(7) can be decreased by a factor of about 200.

*Quasi-steady states at perturbed 2,3-bisphosphoglycerate concentrations*

The existence of a pronounced time-hierarchy causes the occurrence of quasi-steady states. These may appear to the experimenter as true steady states, since the metabolite concentrations change only little during long periods of time. Fig. 7 gives for illustration a plot of [ATP] versus [2,3-bisphosphoglycerate] obtained by numerical integration of the differential equations. From an

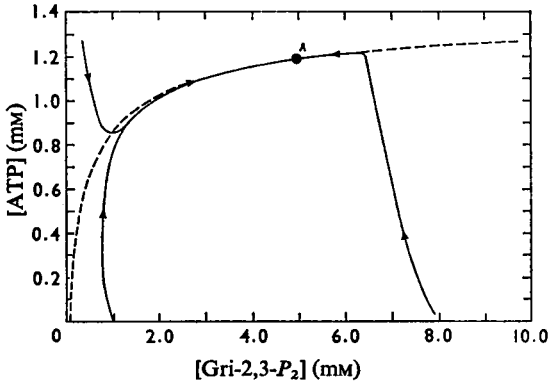


Fig. 7. *Relaxation of ATP and 2,3-bisphosphoglycerate to the steady state*

The continuous lines give the trajectories of the movements from several starting points. The steady state, which is finally approached, is denoted by *A*. The broken line indicates the quasi-stationary state and has been computed by eqns. (4) and (5) by setting the time-derivatives equal to zero.

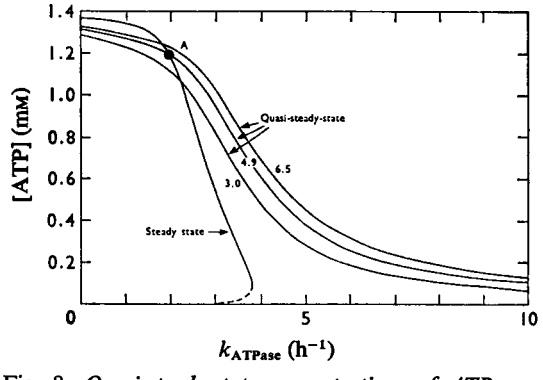


Fig. 8. *Quasi-steady-state concentrations of ATP as a function of the rate constant of the ATPase* ($k_{ATPase}$)

The concentration of 2,3-bisphosphoglycerate was varied as indicated (numbers in mM). The steady-state curve for ATP *in vivo* is given for comparison. It intersects the quasi-steady-state curve corresponding to the steady-state concentration of 2,3-bisphosphoglycerate (4.9mM) at the '*in vivo* point' A.

arbitrarily chosen starting point there is initially a fast movement until the system reaches the quasi-steady-state line. This line is determined by the condition that the time-derivatives in eqns. (4) and (5) are zero. The system now moves on the quasi-steady-state line slowly until the true steady state is reached. The slow movement is determined by the relaxation of 2,3-bisphosphoglycerate. It takes the glycolytic system about 0.5–2h to approach the quasi-steady state, whereas the subsequent slow movement takes more than 10h. Since most experiments cover the first time-period the existence of the quasi-steady state is of practical importance.

Fig. 8 shows the quasi-steady-state solutions of ATP as a function of the rate constant of the ATP-consuming processes. The curves were calculated by setting eqns. (4) and (5) equal to zero. The 2,3-bisphosphoglycerate concentration serves as a parameter of this system. For comparison, the steady-state curve *in vivo* is plotted. The quasi-steady state has only one stable solution. The variation of the 2,3-bisphosphoglycerate concentration has relatively little influence on the ATP concentration. Changes of 2,3-bisphosphoglycerate as large as 2mM affect the ATP concentration by less than 5%. Therefore the metabolite concentrations remain relatively constant during the quasi-steady-state period even for large changes in [2,3-bisphosphoglycerate]. Comparison of the curves in Fig. 8 shows that ATP is more constant in the quasi-steady state than it is in the steady state *in vivo*. This means that the glycolytic system can tolerate ATP overconsumption for a short time better than it can do for longer periods of time. Two mechanisms are responsible for the constancy of the ATP concentration in quasi-steady states. One is the effect of 'energy buffering' discussed under '2,3-Bisphosphoglycerate by-pass acting as an energy buffer' for transitions between steady states *in vivo*. A second mechanism is the formation of ATP in the reaction of the pyruvate kinase at the expense of 2,3-bisphosphoglycerate. Whereas in the true steady-state formation and degradation of 2,3-bisphosphoglycerate are always equal, in the quasi-steady state more 2,3-bisphosphoglycerate is degraded than formed. The second mechanism is responsible for the flatter curve of ATP in quasi-steady states than in steady states *in vivo*.

### *Control properties of the quasi-steady state at perturbed 2,3-bisphosphoglycerate concentrations*

The values of the control strengths and control matrices calculated for the quasi-steady state are given in Table 9. Generally the enzymes have less influence on the metabolite concentrations in the quasi-steady state as compared with the true steady state. The signs of the elements of the matrices coincide, except for 2,3-bisphosphoglycerate phosphatase, which in the quasi-steady state has a positive influence on ATP and phosphoenolpyruvate. This is due to the fact that its activity determines the additional flux via pyruvate kinase. As Table 9 reveals, the flux control in the quasi-steady state is exerted almost entirely by the hexokinase–phosphofructokinase system. The explanation is that ATP is

practically uninfluenced by the activities of the enzymes so that no significant feedback to the first enzymes exists.

The results for the quasi-steady states at perturbed 2,3-bisphosphoglycerate concentrations correspond essentially to those of our previous model (Rapoport *et al.*, 1974). In both models the ATP concentration is uninfluenced by the glycolytic enzymes, so that it acts as an outer parameter of the system. Consequently, in both models the flux control is exerted by the first two irreversible enzymes. Further, as Table 9 reveals, phosphoenolpyruvate is approximately proportional to the glycolytic flux, as in the previous model (Rapoport *et al.*, 1974). At variance with the earlier model phosphoenolpyruvate is affected by the enzymes of the by-pass and by the ATPases. In the quasi-steady-state model pyruvate kinase has a comparatively weak influence on phosphoenolpyruvate.

*Experimental tests of the quasi-steady-state solutions at perturbed 2,3-bisphosphoglycerate concentrations*

*Prediction of metabolite changes produced by outer effectors.* For the data selected in Table 10 (Jacobasch, 1968, 1970; Jacobasch *et al.*, 1972, 1974) it was assumed that a quasi-steady state had been reached. Although the data refer to conditions *in vitro* they are suitable for testing the model *in vivo*. This is due to the high pyruvate concentration used in these particular experiments (see 'The system of glycolysis *in vitro*' section). It is apparent from Table 10 that good agreement is obtained assuming that only the hexokinase–phosphofructokinase system is activated by high $P_i$ or $NH_4^+$ concentrations. This confirms previous results, which showed that phosphofructokinase is the main interaction site with these effectors (Rapoport *et al.*, 1974).

*Measurement of the control strengths.* Table 11 summarizes some experimental data obtained in our institute (Reimann *et al.*, 1975). Purified enzymes were added to a concentrated haemolysate which displayed stable concentrations of ATP and other metabolites for at least 1 h. The qualitative agreement with the theoretical expectations is satisfactory. Pyruvate kinase and glyceraldehyde phosphate dehydrogenase had no influence on glucose consumption and lactate production. Hexokinase and phosphofructokinase exerted a positive flux control.

*Description of a time-dependent process; addition of glucose to starved erythrocytes.* Fig. 9 gives experimental points on the addition of glucose to glucose-depleted erythrocytes (Tomoda & Minakami, 1975). The curves represent computer simulations using parameter values almost identical with those best fitting the steady-state data *in vivo* at pH 7.2 (Table 2). The agreement of theoretical and experimental values demonstrates that the model can describe time-dependent changes. The most important feature of the curves is the occurrence of the predicted quasi-steady state at perturbed 2,3-bisphosphoglycerate concentrations. Phosphoenolpyruvate and the adenine nucleotides reach almost constant concentrations after about 0.5 h.

Table 9. *Control matrices and control strengths for the quasi-steady states at perturbed concentrations of* 2,3-*bisphosphoglycerate*

| Enzyme | ATP | Phosphoenol-pyruvate | Flux (C) |
|---|---|---|---|
| Hexokinase–phospho-fructokinase system | 0.61 | 1.37 | 1.09 |
| ATPase | −0.21 | −0.75 | −0.11 |
| Pyruvate kinase | 0.10 | −0.52 | 0.05 |
| Bisphosphoglycerate mutase | −0.10 | −0.43 | −0.05 |
| 2,3-Bisphosphoglycerate phosphatase | 0.05 | 0.33 | 0.02 |

Table 10. *Prediction of some metabolite concentrations in a quasi-steady state at perturbed concentrations of* 2,3-*bisphosphoglycerate*

The total sum of adenine nucleotides was held constant at 1.4 mM. $V_{max.}$ was increased by a factor of 1.3 for $P_i$ addition and by a factor of 1.2 for $NH_4^+$ addition. 2,3-Bisphosphoglycerate was 5.5 mM for the experiment of $P_i$ addition and 4.5 mM for $NH_4^+$ addition. The experimental data were taken from Jacobasch (1968, 1970) and Jacobasch *et al.* (1972, 1974). The concentrations are given in $\mu$M, the flux in $\mu M \cdot h^{-1}$.

| Metabolite | Addition of 50 mM-$P_i$ (37°C, pH 7.2, 1 h incubation) | | Addition of 28 mM-$NH_4^+$ (37°C, pH 7.2, 1 h incubation) | |
|---|---|---|---|---|
| | Theoretical | Experimental | Theoretical | Experimental |
| ATP | 1240 | 1285 | 1211 | 1255 |
| ADP | 132 | 131 | 152 | 86 |
| Phosphoenolpyruvate | 39 | 32 | 32 | 27 |
| Glycolytic flux (Δ[glucose]) | 1936 | 1800 | 1764 | 1600 |

Table 11. *Effects of added enzymes on the flux in haemolysates*

The haemolysates were prepared by ultrasonication (Reimann *et al.*, 1975). ATP and the glycolytic flux were constant for at least 1 h. Purified enzymes were added to double the concentrations. The enzymes were from the following sources: pyruvate kinase and phosphofructokinase, rabbit muscle; glyceraldehyde phosphate dehydrogenase, human erythrocytes; hexokinase, yeast.

| Enzyme added | Δ[Glucose] (mM·h$^{-1}$) | Δ[Lactate] (mM·h$^{-1}$) |
|---|---|---|
| Control | 1.2±0.2 | 2.4±0.2 |
| Pyruvate kinase | 1.2 | 2.5 |
| Glyceraldehyde phosphate dehydrogenase | 1.1 | 2.3 |
| Phosphofructokinase | 1.7 | 3.4 |
| Hexokinase | 1.6 | 2.9 |

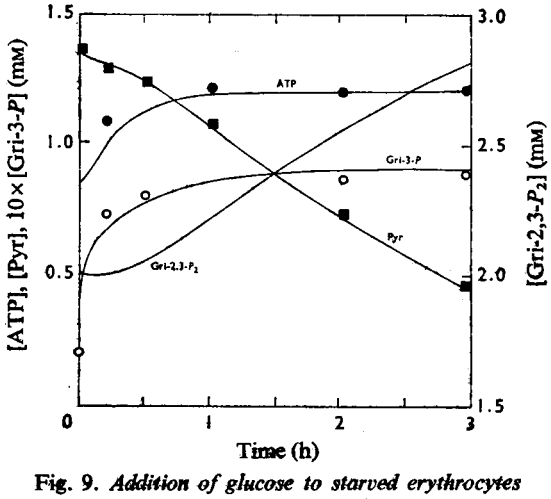


Fig. 9. *Addition of glucose to starved erythrocytes*

Erythrocytes were preincubated for 2h at pH7.6 in the absence of glucose. Then glucose was added and the time-dependent changes of the metabolite concentrations were measured. The points in the Figure represent experimental values (Tomoda & Minakami, 1975), the curves were calculated. The parameter values given in Table 2 were used with the following exceptions: $k_{PyrK} = 0.4\,\mu M^{-1}\cdot h^{-1}$, $k_{Gri\text{-}P_2M} = 5\times10^4 h^{-1}$, $k_{ATPase} = 2.65 h^{-1}$, $A = 1500\,\mu M$. For the hexokinase–phosphofructokinase system ATP was assumed to be saturating and $V_{max.}$ was adjusted to give the experimental glycolytic flux ($V_{max.} = 4300\,\mu M\cdot h^{-1}$). Experimental values for 2,3-bisphosphoglycerate were not given for this experiment, and therefore a starting value of 2 mM was assumed. A conservation sum T of 3450 $\mu$M was used. Its value is not critical, however, during the first hours of incubation where pyruvate is high. Beyond 0.5 h a quasi-steady-state period is observed for ATP and 3-phosphoglycerate, but 2,3-bisphosphoglycerate and consequently pyruvate change continuously. The 2,3-bisphosphoglycerate changes were recently observed experimentally and show qualitatively the expected behaviour (S. Minakami, personal communication).

**The System of Glycolysis *in vitro***

Conditions *in vitro* are defined as incubations of erythrocytes in test tubes where the cells are investigated in an isolated state. Details of the experimental conditions are cited under 'Experimental tests of the quasi-steady-state conditions at perturbed 2,3-bisphosphoglycerate concentrations'.

For the conditions *in vivo* the concentrations of pyruvate and lactate, which are determined by other tissues of the body, have no influence on the 'core' of glycolysis, i.e. on the energy metabolism (see under 'Steady-state equations and general features of the solutions'). *In vitro*, however, one has a closed system in which lactate and pyruvate are not exchanged and for which the conservation restriction for the oxidized metabolites holds (Rapoport *et al.*, 1974):

$$T = [NAD^+] + [Gri\text{-}1,3\text{-}P_2] + [Gri\text{-}2,3\text{-}P_2] + [Gri\text{-}3\text{-}P] + [Gri\text{-}2\text{-}P] + [Prv\text{-}P] + [Pyr] \quad (18)$$

where T is the conservation quantity for the oxidized metabolites. Since pyruvate is a constituent of this sum it is expected that its variation will cause compensatory changes in the concentrations of the other metabolites. Further, since lactate accumulates *in vitro*, this could lead to time-dependences of other metabolites so that time-independent states might be impossible even for parts of the glycolytic system.

The following theoretical considerations demonstrate (1) that quasi-steady states occur *in vitro* for all metabolites except for lactate, fructose 1,6-bisphosphate and triose phosphate, and (2) that the conservation sum T influences the concentrations of the metabolites and the relaxation time of the system.

*Differential equations for the closed system*

For the closed system *in vitro* the term for the exchange of lactate and pyruvate must be omitted from eqn. (7). In eqn. (4) the concentrations of fructose 1,6-bisphosphate and triose phosphate can be expressed by the concentrations of phosphoenolpyruvate, ATP, ADP and lactate:

$$\frac{d}{dt}\left[\left(\frac{Q_1[Prv\text{-}P][ATP][Lac]}{[ADP][Pyr]} + [Gri\text{-}1,3\text{-}P_2] + Q_2[Prv\text{-}P]\right)\right] = 2v_{HK-PFK} - v_{Gri\text{-}P_2M} + v_{Gri\text{-}2,3\text{-}P_2ase} - v_{PyrK} \quad (19)$$

with

$$Q_1 = \frac{1 + \frac{2}{q_{Ald}} + \frac{1}{q_{TIM}}}{q_{Gri\text{-}PK}\,q_{Gri\text{-}PM}\,q_{Enol}\,q_{Gra\text{-}PD}\,q_{LacD}}$$

$$Q_2 = 1 + \frac{1}{q_{Enol}} + \frac{1}{q_{Enol}\,q_{Gri\text{-}PM}} \quad (20)$$

By use of the conservation eqns. (2) and (18) the time-derivative of pyruvate can be expressed in terms of phosphoenolpyruvate, 2,3-bisphosphoglycerate, 1,3-bisphosphoglycerate and nicotinamide nucleotides. Eqn. (7) becomes:

$$\frac{d[Lac]}{dt} = v_{PyrK} + \frac{1-Y_1}{1+\frac{[Pyr]}{[Lac]}Y_1}\left(Q_2\frac{d[Prv\text{-}P]}{dt} + \frac{d[Gri\text{-}2,3\text{-}P_2]}{dt} + \frac{d[Gri\text{-}1,3\text{-}P_2]}{dt}\right) \quad (21)$$

where

$$Y_1 = \frac{[NAD^+][NADH]}{[NAD^+][NADH]+[Pyr]\cdot N} \quad (22)$$

Differentiation of the left-hand side of eqn. (19) yields, after some rearrangements

$$\frac{d[Gri\text{-}1,3\text{-}P_2]}{dt} + (Q_2+F_1)\frac{d[Prv\text{-}P]}{dt} = 2v_{HK-PFK} - v_{Gri\text{-}P_2M} + v_{Gri\text{-}2,3\text{-}P_2ase} - v_{PyrK}(1+F_2) - F_3\frac{d[ATP]}{dt} - F_4\frac{d[Gri\text{-}2,3\text{-}P_2]}{dt} \quad (23)$$

with

$$F_1 = \frac{Q_1[ATP]}{[ADP][Pyr]}\left[[Lac]+[Prv\text{-}P]\left(Q_2 + \frac{[ATP](1-Y_1)([Lac]+[Pyr])}{q_{Enol}q_{Gri\text{-}PM}q_{Gri\text{-}PK}[ADP]([Lac]+[Pyr]Y_1)}\right)\right] \quad (24a)$$

$$F_2 = \frac{Q_1[Prv\text{-}P][ATP][Lac](1-Y_1)}{[ADP][Pyr]([Lac]+[Pyr]Y_1)} \quad (24b)$$

$$F_3 = \left[1-\left(\frac{d[ADP]}{d[ATP]}\frac{[ATP]}{[ADP]}\right)\right]\frac{Q_1[Prv\text{-}P]}{[ADP][Pyr]}\left[[Lac] + \frac{[Prv\text{-}P][ATP](1-Y_1)([Lac]+[Pyr])}{q_{Enol}q_{Gri\text{-}PM}q_{Gri\text{-}PK}[ADP]([Lac]+[Pyr]Y_1)}\right] \quad (24c)$$

$$F_4 = \frac{Q_1[Prv\text{-}P][ATP](1-Y_1)([Lac]+[Pyr])}{[ADP][Pyr]([Lac]+[Pyr]Y_1)} \quad (24d)$$

Eqn. (23) differs from the corresponding '*in vivo*' eqn. (4) by the occurrence of terms $F_1$–$F_4$. At pH 7.2, assuming normal metabolite concentrations, the terms have the following numerical values: $F_1 = 2.8$; $F_2 = 0.033$; $F_3 = 0.21$; $F_4 = 0.35$. Most of these quantities are not small enough to be neglected. Their magnitude can be decreased by high concentrations of pyruvate (eqn. 24). The differential eqns. (5) and (6) for 2,3-bisphosphoglycerate and ATP remain unchanged for the situation *in vitro*.

Obviously, the system *in vitro* has no steady-state solution, in contrast with that *in vivo*, since eqn. (21) cannot be set equal to zero; lactate increases steadily.

*Existence of quasi-steady states in the closed system for all glycolytic metabolites except for lactate, fructose 1,6-bisphosphate and triose phosphate*

The following considerations demonstrate the existence of quasi-steady states *in vitro*. Setting the time-derivatives in the differential eqn. (23) equal to zero, one obtains an equation similar to that for the steady state *in vivo* (eqn. 8), with the difference that it contains the term $F_2$:

$$2v_{HK-PFK} - v_{Gri\text{-}P_2M} + v_{Gri\text{-}2,3\text{-}P_2ase} - v_{PyrK}(1+F_2) = 0 \quad (25)$$

If $F_2$ were constant a steady state could be expected for the adenine nucleotides, phosphoglycerates and for pyruvate (see eqns. 5, 6 and 18). The constancy of $F_2$ depends on the term

$$Y_2 = \frac{[Pyr]N}{[NAD^+][NADH]+[Pyr]N} \quad (26)$$

which is influenced by the concentrations of the nicotinamide nucleotides. By use of the equilibria (1) and the conservation eqn. (2) the following expression is obtained for $[NAD^+]$:

$$[NAD^+] = \frac{N}{1+\frac{[Lac]}{[Pyr]q_{LacD}}} \quad (27)$$

Since *in vitro* lactate increases steadily the concentration of $NAD^+$ decreases and consequently the term $Y_2$ cannot be constant. However, if the condition $NAD^+ \gg NADH$ (or vice versa) is fulfilled the influence of the time-dependent changes of this system is negligible ($Y_2$ tends to unity). For erythrocytes at pH 7.2 $NAD^+$ is always much higher than NADH, so that $F_2$, and consequently the adenine nucleotides and phosphoglycerates, may be approximately constant. Pyruvate is also time-independent, owing to the conservation sum for the oxidized metabolites. The case of $NAD^+ \ll NADH$ can only be expected if lactate tends to infinity.

The computer curves shown in Fig. 10 verify these conclusions. Metabolites which are not influenced *in vivo* by the exchange of lactate and pyruvate reach constant values *in vitro* too.

The accumulation of lactate is accompanied by an increase in fructose 1,6-bisphosphate and triose phosphate. This is explained by the coupling of the lactate dehydrogenase and glyceraldehyde phosphate dehydrogenase by the nicotinamide nucleotides which leads to the following relation (cf. eqn. 1):

$$[Gra\text{-}3\text{-}P] = \frac{[Gri\text{-}1,3\text{-}P_2][Lac]}{q_{LacD}q'_{Gra\text{-}PD}[Pyr]} \quad (28)$$

where 1,3-bisphosphoglycerate and pyruvate are constant with time. Since part of the flux from the

hexokinase–phosphofructokinase system is used to accumulate fructose 1,6-bisphosphate and triose phosphate, the glucose consumption must be higher than the corresponding lactate formation. The quasi-stationary character of the state shown in Fig. 10 is apparent from the slow decrease of [$NAD^+$].

*Comparison of the concentrations of the metabolites in a quasi-steady state with those in the steady state in vivo; limitations by the amounts of oxidation equivalents*

The differences in the concentrations of the adenine nucleotides and phosphoglycerates in the quasi-steady state from those *in vivo* depend only on the magnitude of the term $F_2$ (eqn. 25). At pH7.2 only small deviations from the conditions *in vivo* are calculated (see value given above). However, for transient processes the differences are greater, since the other terms of eqn. (23) may not be neglected.

For the limiting case of infinite pyruvate concentrations there are no constraints imposed by oxidation equivalents, and $F_2$, as well as the accumulation rate of fructose 1,6-bisphosphate and triose phosphate, tend to zero. Consequently, the adenine nucleotides and phosphoglycerates attain the values *in vivo*. Even their time-dependent behaviour is identical with that *in vivo* if the pyruvate concentration is infinite, since all terms which may cause deviations (cf. eqn. 24) become vanishingly small. This situation was approximated in all experiments discussed under 'Experimental tests of the quasi-steady-state solutions at perturbed 2,3-bisphosphoglycerate concentrations'.

The restriction by the conservation quantity for the oxidized metabolites becomes more apparent if the hexokinase–phosphofructokinase system is activated (Table 12). Whereas in the unconstrained system *in vivo* 2,3-bisphosphoglycerate and the other oxidized phosphoglycerates would increase greatly, the changes are limited *in vitro* by the amount of oxidation equivalents available in the system. The increase in 2,3-bisphosphoglycerate is compensated for mainly by a decrease in pyruvate. This in turn leads to a higher rate of accumulation of fructose 1,6-bisphosphate and triose phosphate (eqn. 28). The increased flux through hexokinase and phosphofructokinase results in a more pronounced discrepancy between glucose consumption and lactate formation. Under such conditions ATP may even decrease, despite a higher glucose consumption. The accumulation of fructose 1,6-bisphosphate and triose phosphate may be regarded as a 'futile cycle' which buffers changes in ATP. This is an effect similar to that described for the 2,3-bis-

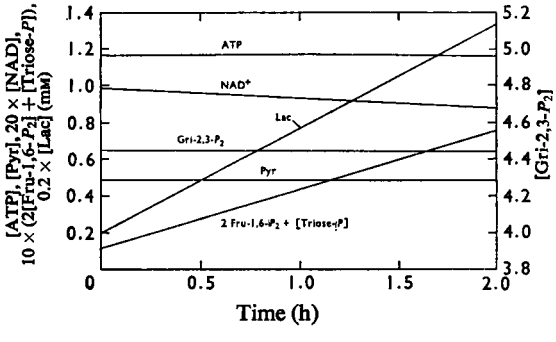


Fig. 10. *Quasi-steady-state behaviour in vitro of the glycolytic metabolites*

Quasi-steady states are obtained *in vitro* for all metabolites except for lactate, fructose 1,6-bisphosphate and triose phosphate. The slow decrease of $NAD^+$ may be seen. A conservation sum T of 5mM was assumed. For $Q_1$ a value of $3.6\times10^{-2}$ was used, which is deduced from the individual equilibrium constants (see eqn. 22). N was set at 50$\mu$M.

Table 12. *Restriction of metabolite changes by the conservation equation for the oxidized metabolites*

The hexokinase–phosphofructokinase system was activated by a factor of 2 (increase of $V_{max.}$ from 3170 to 6340$\mu$M·$h^{-1}$). ΔFlux is the difference between the rates of glucose consumption and lactate formation given in triose units ($\mu$M·$h^{-1}$). The concentrations are given in $\mu$M.

| | Conservation sum | | | | | | | |
|---|---|---|---|---|---|---|---|---|
| | T = ∞ | | T = 6.0mM | | T = 5.0mM | | T = 4.5mM | |
| Metabolite | Control | Activated | Control | Activated | Control | Activated | Control | Activated |
| ATP | 1186 | 1354 | 1176 | 1179 | 1162 | 1133 | 1149 | 1103 |
| 2,3-Bisphosphoglycerate | 4900 | 29470 | 4690 | 5838 | 4438 | 4872 | 4183 | 4390 |
| Phosphoenolpyruvate | 26.3 | 215.6 | 25.2 | 39.2 | 23.8 | 32.2 | 22.4 | 29.1 |
| Pyruvate | ∞ | ∞ | 1204 | 29.4 | 482 | 19.6 | 245 | 15.4 |
| ΔFlux | 0 | 0 | 14.6 | 1261 | 33.2 | 1436 | 57.2 | 1557 |

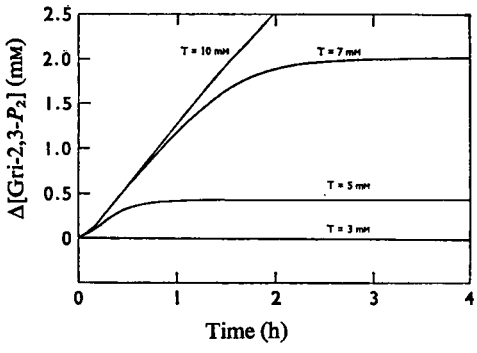


Fig. 11. *Relaxation of 2,3-bisphosphoglycerate after a twofold activation of the hexokinase–phosphofructokinase system at different concentrations of the oxidation equivalents*

$\Delta$[Gri-2,3-$P_2$] is defined as [Gri-2,3-$P_2$]($t$)−[Gri-2,3-$P_2$]($t=0$). The starting values for 2,3-bisphosphoglycerate [Gri-2,3-$P_2$($t=0$)] depend on the conservation sum T. The transition times $T_{Gri\text{-}2,3\text{-}P_2}$ were calculated by use of the expression

$$T_{Gri\text{-}2,3\text{-}P_2} = \frac{\int_0^{t_c} (t\Delta[\text{Gri-2,3-}P_2])\,dt}{\int_0^{t_c} (\Delta[\text{Gri-2,3-}P_2])\,dt}$$

(Heinrich & Rapoport, 1975) at different sums of the oxidation equivalents. For $T=10$, 7 and 5mM the $T_{Gri\text{-}2,3\text{-}P_2}$ values were 1.29, 0.66 and 0.21h respectively. For the upper limits, $t_c$, of the integrals such times were chosen where the deviations of the 2,3-bisphosphoglycerate concentrations from their steady-state values fell below 2% of the final concentration. This corresponds to the experimental error for the determination of this metabolite. Therefore no relaxation of 2,3-bisphosphoglycerate could be observed experimentally for the lowest conservation sum T = 3mM.

phosphoglycerate by-pass (see under '2,3-Bisphosphoglycerate by-pass acting as an energy buffer').

Fig. 11 gives the time-dependent changes in 2,3-bisphosphoglycerate for different values of the conservation quantity T after activation of the hexokinase–phosphofructokinase system. The final concentration of 2,3-bisphosphoglycerate decreases if the conservation sum is lowered (cf. Table 12) and the time needed for the attainment of constant 2,3-bisphosphoglycerate concentrations becomes shorter. This is explained by the circumstance that the initial velocities differ little in the face of fairly large variations in the final 2,3-bisphosphoglycerate concentrations. Therefore the relaxation time of the system, which is around 15h *in vivo*, decreases to about 1h for T=10mM, and for an activation of the glucose consumption by a factor of about 2 (Fig. 11).

It may be concluded that the attainment of quasi-steady states for all glycolytic metabolites except for lactate, fructose 1,6-bisphosphate and triose phosphate can be observed in the closed system during the short incubation periods *in vitro* only if the conservation sum T is sufficiently small. If the sum T is large, 2,3-bisphosphoglycerate remains unrelaxed for long periods of time. Under these conditions the quasi-steady state *in vivo* discussed under 'Quasi-steady states at perturbed 2,3-bisphosphoglycerate concentrations' may be observed.

## General Discussion

Our approach to set up a model was guided by the following principles. First, the comparison of theoretical and experimental results is essential for model building, verification and predictions (Garfinkel *et al.*, 1970). Secondly, the model should involve as few parameters and variables as possible (Higgins, 1967; Sel'kov, 1968; Reich & Sel'kov, 1974). Their number is determined by the requirement that they should suffice to represent real experiments. Thirdly, the system as a whole has to be considered, not parts or single steps.

The agreement of theory and experiments indicates that the most important interactions between metabolites and enzymes and the essential stoicheiometric relations are included in our model. Omission of any of the important interactions or stoicheiometries lead to discrepancies with the experimental data. Thus it appears that the present model is the simplest one compatible with an adequate description of the glycolytic system.

The analysis of this model shows that only four essential variables are sufficient to characterize the system. From the standpoint of experimental convenience these may be ATP, 2,3-bisphosphoglycerate, 3-phosphoglycerate and lactate. Of course, there may be substitutions, such as AMP or ADP for ATP, phosphoenolpyruvate, 2-phosphoglycerate or 1,3-bisphosphoglycerate for 3-phosphoglycerate or the glycolytic flux for lactate. Compared with the previous proposal (Rapoport *et al.*, 1974), glucose 6-phosphate is omitted, since it is only of importance for the elucidation of the interrelations between hexokinase and phosphofructokinase. The additional variables are ATP and 2,3-bisphosphoglycerate, the importance of which has become clarified by the present analysis. The analysis also reconfirms the previous conclusions (Rapoport *et al.*, 1974) that in the steady state the equilibrium enzymes phosphoglycerate kinase and glyceraldehyde phosphate dehydrogenase have no influence on either flux or metabolites of glycolysis, whereas pyruvate kinase, which does affect some intermediates, has little influence on the flux. This is in contrast with various intuitive assumptions (Reinauer & Bruns,

1964; Minakami, 1968). It should be emphasized that the role of an enzyme under steady-state conditions must be distinguished from that in a transient process. Enzymes with high control strengths need not control a transient process, and vice versa. This is illustrated by the fact that the 2,3-bisphosphoglycerate phosphatase, which has only a small control strength (cf. Table 5), exerts a strong influence on transient processes.

So far the role of the ATP-consuming processes in regulating the glycolysis has been largely neglected in both theoretical and experimental work. From the present study it emerges, however, that ATP-consuming processes are of great importance.

Some principles of the regulation of the important metabolite ATP are revealed. ATP is kept approximately constant in the cell by three mechanisms. First, the 2,3-bisphosphoglycerate by-pass acts as an energy buffer, so that a change in ATP consumption is compensated for by a variation in the waste of ATP by the by-pass. Secondly, the metabolite 2,3-bisphosphoglycerate acts as an energy source, as it may yield ATP for a certain period of time at the pyruvate kinase step in case of ATP over-consumption. A third mechanism is observed *in vitro*, where ATP changes can be buffered by variations in the accumulation rate of fructose 1,6-bisphosphate and triose phosphate. The first and third mechanisms are regulators of energy-consuming processes, whereas the second one refers to an energy-producing process.

An unexpected biological phenomenon has turned up, i.e. that the ATP-consumption rate assumes its maximal value at the steady state *in vivo*. This holds for various species independent of their values of 2,3-bisphosphoglycerate, ATP or glycolytic flux. It appears as if, given the need for ATP consumption, the whole glycolytic system is composed in such a manner as to yield maximal efficiency. This must represent an evolutionary adaptation which involves the whole set of elements which constitute the glycolytic system, rather than one single factor. It appears strange, however, that any activation of the ATPases should produce a lowered ATP consumption unless the parameters of the glycolytic enzymes are changed by outer effectors, such as $H^+$, $P_i$ or $NH_4^+$ ions. Possibly erythrocytes are not faced with great changes in their need for ATP. In this respect erythrocytes are not representative of other cells, which are geared for great changes in their need for ATP, e.g. those of muscle. In these cells glycogenolysis is highly sensitive to the breakdown products of ATP, namely AMP and $P_i$, so that a stronger response to changes in the ATP consumption exists. A preliminary modelling of such a system indicates that the rate of ATP consumption may vary over a wide range (R. Heinrich & T. A. Rapoport, unpublished work). A similar behaviour is shown by the erythrocyte system during periods of time in which a quasi-steady state obtains. An activation of the ATPase may lead to an increased ATP consumption for several hours.

The fundamental difference shown in this paper between the conditions *in vivo* and *in vitro* has been largely neglected in the past. So far there has been no general appreciation of the extent to which the situation of cells *in vitro* corresponds to that *in vivo* and no means of setting up experiments *in vitro* to approximate to the conditions *in vivo*. Whereas a steady state exists *in vivo* to a high degree of approximation, it cannot be realized *in vitro*. Within certain periods of incubation, i.e. between about 0.5 and 2h, a quasi-steady state may be achieved, a condition which is favourable for both theoretical and experimental analysis. Two kinds of quasi-steady states can be observed *in vitro*. One can be reached during the short incubation periods for all glycolytic metabolites except for lactate, fructose 1,6-bisphosphate and triose phosphate at low amounts of oxidation equivalents. Theoretically the same quasi-steady state is also possible for high values of the conservation sum, but its attainment would require a long time. A second type of quasi-steady state, which is limited to adenine nucleotides and phosphoglycerates, is defined by unrelaxed 2,3-bisphosphoglycerate concentrations. This kind of quasi-steady state may also occur *in vivo* whenever 2,3-bisphosphoglycerate is not in a steady state, such as during acidosis or exposure to high altitude (Guest & Rapoport, 1939; Torrance *et al.*, 1969; Hamasaki *et al.*, 1974). The quasi-steady-state conditions *in vivo* may be simulated *in vitro* by provision of high pyruvate concentrations.

The theoretical investigation points also to the importance of the washing procedure of the cells preceding their incubation. The cells should be washed at conditions close to those *in vivo*, i.e. at 37°C, pH7.4 (extracellular), 1mM-$P_i$, 0.2–0.3mM-pyruvate and high glucose concentrations. Deviating conditions may cause undefined non-steady-state conditions at the beginning of the incubation, as seems to be the case for most experiments *in vitro* so far performed. For instance, pyruvate is found experimentally at pH7.2 below 0.2mM, whereas the theoretical steady-state value is much higher (Table 10).

A pure steady-state treatment has its limitation. This is shown by the existence of quasi-steady states, of unstable states and by the structural instability (see the Appendix), which may be of general importance if conservation sums are involved in the model. These features cannot be found by algebraic equations which yield only the steady-state solutions. An investigation of the local stability properties and of the dynamic behaviour is a necessary supplement of such a treatment.

The analysis revealed a pronounced time-hierarchy of the glycolytic reactions of erythrocytes which is mainly due to the slow 2,3-bisphosphoglycerate phosphatase reaction. For the investigation of the hierarchical structure of a system the eigenvalues seem to be the best representation.

Time-hierarchies are a general feature in nature. Any theoretical or experimental approach requires a confinement of the system to be investigated with respect to the time-ranges. These restrictions determine the experimental methods to be applied as well as the structure of the models assumed. For the present model the lower boundary of time constitutes rapid reactions which were not considered explicitly. These include three types of processes: first, reactions at the level of single enzymes which are usually fast enough to be in a steady state in the metabolic time-range; secondly, glycolytic reactions near to equilibrium; and thirdly, the steady-state aggregation of some enzymes, i.e. of hexokinase and phosphofructokinase. The upper boundary is slow processes such as renewal of the adenine or nicotinamide moieties. By these boundaries the time-range of the model analysed in this paper is set between 1 min and 1–2 days.

**Acknowledgements**

We thank Professor Dr. G. Jacobasch for helpful comments and her and Professor Dr. S. Minakami for the supply of unpublished experimental data. We gratefully acknowledge the help of Mr. M. Otto in some computer work and valuable comments by Dr. G. Willems.

## References

Garfinkel, D., Garfinkel, L., Pring, M., Green, S. B. & Chance, B. (1970) *Annu. Rev. Biochem.* **39**, 473–498

Gerber, G., Berger, H., Jänig, G.-R. & Rapoport, S. M. (1973) *Eur. J. Biochem.* **38**, 563–571

Gerber, G., Preissler, H., Heinrich, R. & Rapoport, S. M. (1974) *Eur. J. Biochem.* **45**, 39–52

Guest, G. M. & Rapoport, S. M. (1939) *Am. J. Dis. Child.* **58**, 1072–1089

Hamasaki, N., Matsuda, Y., Hamano, S., Hara, T. & Minakami, S. (1974) *Clin. Chim. Acta* **50**, 385–395

Harkness, D. R., Thompson, W., Roth, S. & Grayson, V. (1970) *Arch. Biochem. Biophys.* **138**, 208–219

Heinrich, R. & Rapoport, T. A. (1974) *Eur. J. Biochem.* **42**, 89–95

Heinrich, R. & Rapoport, T. A. (1975) *BioSystems* **7**, 130–136

Higgins, J. J. (1965) in *Control of Energy Metabolism* (Chance, B., Estabrook, R. W. & Williamson, J. R., eds.), pp. 13–46, Academic Press, New York and London

Higgins, J. J. (1967) *Ind. Eng. Chem.* **59**, 18–62

Jacobasch, G. (1968) *Folia Haematol.* **89**, 376–391

Jacobasch, G. (1970) Ph.D. Thesis, University of Berlin

Jacobasch, G., Helbig, W., Syllm-Rapoport, I., Pester, H., Heine, K.-M., Boese, Ch., Otto, F. M. & Blau, H.-J. (1969) *Dtsch. Gesundheitswes.* **31**, 144–149

Jacobasch, G., Kühn, B., Gerth, Ch. & Rapoport, S. M. (1972) in *Struktur und Funktion der Erythrocyten* (Rapoport, S. M. & Jung, F., eds.), pp. 297–305, Akademie Verlag, Berlin

Jacobasch, G., Minakami, S. & Rapoport, S. M. (1974) in *Cellular and Molecular Biology of Erythrocytes* (Yoshikawa, H. & Rapoport. S. M., eds.), pp. 55–92, University of Tokyo Press, Tokyo

Kosow, D. P., Oski, F. A., Warms, J. V, B. & Rose, I. A. (1973) *Arch. Biochem. Biophys.* **157**, 114–124

Minakami, S. (1968) in *Metabolism and Membrane Permeability of Erythrocytes and Thrombocytes* (Deutsch, E., Gerlach, E. & Moser, K., eds.), pp. 10–15, Georg Thieme Verlag, Stuttgart

Nakao, M. (1974) in *Cellular and Molecular Biology of Erythrocytes* (Yoshikawa, H. & Rapoport, S. M., eds.), pp. 35–54, University of Tokyo Press, Tokyo

Oski, F. A. & Bowman, H. (1969) *Br. J. Haematol.* **17**, 289–297

Otto, M., Heinrich, R., Kühn, B. & Jacobasch, G. (1974) *Eur. J. Biochem.* **49**, 169–178

Park, D. J. M. (1974) *J. Theor. Biol.* **46**, 31–74

Rapoport, S. M. & Luebering, J. (1950) *J. Biol. Chem.* **183**, 507–516

Rapoport, S. M. & Luebering, J. (1951) *J. Biol. Chem.* **189**, 683–694

Rapoport, T. A., Heinrich, R., Jacobasch, G. & Rapoport, S. M. (1974) *Eur. J. Biochem.* **42**, 107–120

Reich, J. G. & Sel'kov, E. E. (1974) *FEBS Lett.* **40**, *Suppl.*, 119–127

Reimann, B., Küttner, G., Maretzki, D. & Rapoport, S. M. (1975) *Jahrestag. Biochem. Ges. DDR 9th* in the press

Reinauer, H. & Bruns, F. H. (1964) *Biochem. Z.* **340**, 503–521

Rosa, R., Gaillardon, J. & Rosa, J. (1975) *Int. Symp. Strukt. Funkt. Erythrocyten. 7th* (Rapoport, S. M. & Jung, F., eds.), Akademie Verlag, Berlin, in the press

Rose, I. A. & O'Connell, E. L. (1964) *J. Biol. Chem.* **239**, 12–17

Rose, I. A. & Warms, J. V. B. (1970) *J. Biol. Chem.* **245**, 4009–4015

Rose, Z. B. (1968) *J. Biol. Chem.* **243**, 4810–4820

Rose, Z. B. (1973) *Arch. Biochem. Biophys.* **158**, 903–910

Rose, Z. B. & Liebowitz, J. (1970) *J. Biol. Chem.* **245**, 3232–3241

Sel'kov, E. E. (1968) *Eur. J. Biochem.* **4**, 79–86

Sel'kov, E. E. (1975) *Int. Symp. Strukt. Funkt. Erythrocyten. 7th* (Rapoport, S. M. & Jung, F., eds.), Akademie Verlag, Berlin, in the press

Tichonov, A. (1946) *Mat. Sb.* **22**, 193–204

Tomoda, A. & Minakami, S. (1975) *Int. Symp. Strukt. Funkt. Erythrocyten. 7th* (Rapoport, S. M. & Jung, F., eds.), Akademie Verlag, Berlin, in the press

Torrance, J. D., Lefant, C. & Finch, C. A. (1969) *Försvarsmedicin* **5**, 187–191

Willems, J. L. (1973) *Stabilität Dynamischer Systeme*, Oldenbourg Verlag, Munich and Vienna

## APPENDIX

### Variants of the Basic Model

Variants of the basic model are of interest for three reasons. First, some of the elements of the model include assumptions for which alternative structures are conceivable and require exploration. Secondly, the consequences of simplifications need assessment, and thirdly, the extension of the model to glycolysis in other kinds of cells may require some alterations in the model structure. The following discussion is not exhaustive.

*Overall inhibition by ATP of the hexokinase–phosphofructokinase system*

In some kinds of cells an overall inhibition of the hexokinase–phosphofructokinase system with increasing ATP may occur. Typical forms of the resulting curves for [ATP] and the glycolytic flux as functions of the rate constant $k_{ATPase}$ are shown in Appendix Fig. 1. [ATP] is found at a lower constant concentration compared with that in Fig. 2(*a*) of the main text. There is a sharp fall in the ATP concentration at low $k_{ATPase}$ values. The control strength of the ATPase is positive in this model, since a decrease in the ATP concentration leads to flux activation. All other features of the model are the same as those of the basic model.

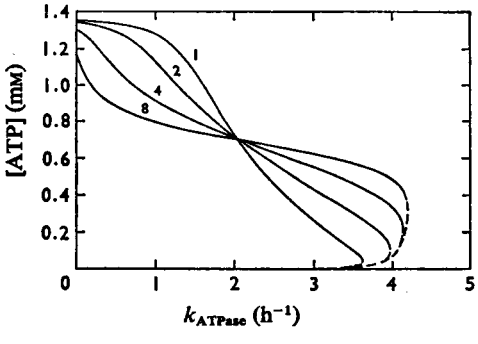


Fig. 1. *ATP concentration and the glycolytic flux as functions of the rate constant of ATPase ($k_{ATPase}$) for an overall inhibition by ATP of the hexokinase–phosphofructokinase system*

For the hexokinase–phosphofructokinase system the following rate law was assumed:

$$v_{HK-PFK} = \frac{V_{max.}\dfrac{[ATP]}{K_m}}{1+\left(\dfrac{[ATP]}{K_i}\right)^n}$$

The values for $V_{max.}$ and $K_m$ are given in Table 2. The value for $K_i$ was 0.7 mM and $n$ was varied as indicated on the curves.

*Inclusion of the inhibition by 2,3-bisphosphoglycerate of hexokinase and phosphofructokinase*

The basic model neglects the inhibitions of hexokinase and phosphofructokinase by 2,3-bisphosphoglycerate (Beutler, 1971; Gerber *et al.*, 1974; Kühn *et al.*, 1974), which may be of some importance. Inclusion of these inhibitions does not change the qualitative form of the curves. Agreement with the experimentally determined concentrations of the metabolites could only be obtained for weak inhibitions by 2,3-bisphosphoglycerate, which are also indicated by studies on the isolated enzymes and on the glycolytic rate at different 2,3-bisphosphoglycerate concentrations (Deuticke *et al.*, 1971).

*Alternative assumptions for the ATP-dependence of the ATPases*

The uncertainties with respect to the rate law of the ATPase have been mentioned in the main paper. Appendix Fig. 2 gives plots of [ATP] versus $k_{ATPase}$ for different rate laws of the ATPases. The ATP-dependence was varied from proportionality to a strong inhibition. The more the values of the first derivatives of the rate laws with respect to [ATP] decrease, the more predominant becomes the unstable part of the curves. Since changes of the glycolytic flux and the ATP concentration of more than 10% are common *in vivo* (I. Rapoport, H. Berger, S. M. Rapoport, R. Elsner & G. Gerber, unpublished work) it is unlikely that the '*in vivo* point' of the

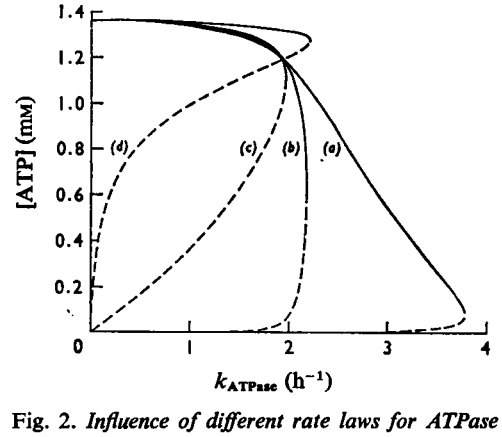


Fig. 2. *Influence of different rate laws for ATPase*

The following rate laws were assumed: curve (*a*) $v_{ATPase}=k_{ATPase}[ATP]$; curve (*b*) $v_{ATPase}=k_{ATPase}\times 2[ATP]/[1+([ATP]/1190)]$; curve (*c*) $v_{ATPase}=k_{ATPase}\times 1190$; curve (*d*) $v_{ATPase}=k_{ATPase}\times 17\cdot 1190/[1+([ATP]/595)]^4$. All rate laws were adjusted to give equal rates at the '*in vivo* point'. Unstable steady states are indicated by broken lines.

system is very near to the bifurcation point. Therefore a positive response to ATP by the ATPases seems more realistic. Rate laws with a positive ATP-dependence but deviating from proportionality (e.g. Michaelis functions) do not modify the qualitative structure of the basic model. In particular, the optimum location of the '*in vivo* point' in Fig. 5 of the main text remains unchanged regardless of the rate law assumed for the ATPases.

*Inclusion of synthesis and breakdown of adenine nucleotides*

The characteristic times of these processes are in the range of 10 days (Lowy *et al.*, 1958), i.e. they are much slower than all processes of the basic model. The following considerations show that the form of the steady-state curves for ATP changes qualitatively if the metabolism of the adenine moiety is included. The following differential equation for synthesis and breakdown of adenine nucleotides can be written:

$$\frac{dA}{dt} = v_{synthesis} - v_{breakdown}$$

Only if $v_{synthesis}$ and $v_{breakdown}$ are zero is there obtained a conservation restriction. For any value of $v_{synthesis}$ and $v_{breakdown}$ greater than zero an integration constant cannot be obtained. The transition from one steady state to another can result in great variations of the sum of adenine nucleotides even if the rate of changes may be very slow. One may call this a 'structural instability' of the model.

In Appendix Fig. 3 two steady-state curves of [ATP] versus $k_{ATPase}$ are shown based on simple rate expressions for $v_{synthesis}$ and $v_{breakdown}$. The curves tend to infinity when $k_{ATPase}$ reaches a lower critical value. The ATP concentration displays a relatively strong dependence on the ATP consumption. These features differ from those obtained if a conservation sum exists for the adenine nucleotides. From the rates of renewal of adenine nucleotides one may estimate the validity of the steady-state model *in vivo* to be limited to a time-period up to 1–2 days.

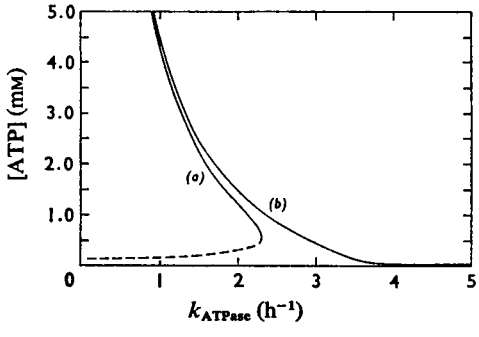


Fig. 3. *ATP concentration as a function of the rate constant of the ATPase ($k_{ATPase}$) for a system which includes synthesis and breakdown of adenine nucleotides*

The two curves were calculated on the basis of different assumptions with respect to the rate laws of synthesis and breakdown of adenine nucleotides. curve (*a*): $v_{synthesis} = \rho \cdot v_{HK-PFK}$ ($\rho$ is a constant factor); $v_{breakdown} = k_{AMP} \times [AMP]$. The ratio $\rho/k_{AMP}$ was arbitrarily chosen to be 0.05 h. A constant fraction of the glycolytic flux was assumed to be used for synthesis of the adenine moiety. Curve (*b*): $v_{synthesis} = 317\,\mu M \cdot h^{-1}$; $k_{AMP} = 0.2\,h^{-1}$. The numerical values were arbitrarily chosen. A constant flux of synthesis of the adenine moiety was assumed. AMP degradation was set proportional to [AMP].

## References

Beutler, E. (1971) *Nature (London) New Biol.* **232**, 20–25
Deuticke, B., Duhm, J. & Dierkesmann, R. (1971) *Pflügers Arch.* **326**, 15–34
Gerber, G., Preissler, H., Heinrich, R. & Rapoport, S. M. (1974) *Eur. J. Biochem.* **45**, 39–52
Kühn, B., Jacobasch, G., Gerth, Ch. & Rapoport, S. M. (1974) *Eur. J. Biochem.* **43**, 443–450
Lowy, B. A., Ramot, B. & London, I. M. (1958) *Nature (London)* **181**, 324–326